Electron Interactions with C_2F_6

L. G. Christophorou and J. K. Olthoff

Electricity Division, Electronics and Electrical Engineering Laboratory, National Institute of Standards and Technology, Gaithersburg, Maryland 20899-0001

Received August 18, 1997; revised manuscript received October 28, 1997

Perfluoroethane (C_2F_6, hexafluoroethane) is a man-made gas with many important applications (e.g., in the aluminum industry, the semiconductor industry, plasma chemistry and etching technologies, and pulsed power switching). In these and other uses, knowledge of the interactions of slow electrons (kinetic energies less than about 100 eV) is fundamental in optimizing performance parameters involved in the particular application. We, therefore, have critically evaluated and synthesized existing knowledge on electron interactions with C_2F_6. The following cross sections and their intercomparison are presented and discussed: total electron scattering, momentum transfer, integral elastic, differential elastic, differential vibrational, vibrational inelastic, total ionization, partial ionization, total dissociation, and electron attachment. Information is presented also on the coefficients for electron impact ionization, effective ionization, electron attachment, and electron transport (lateral diffusion coefficient and drift velocity), as well as on the rate constant for electron attachment as a function of the mean electron energy and gas temperature. While some information is available for these cross sections, additional measurements are needed for each of them, especially for inelastic electron scattering and momentum transfer. No published data are available for dissociation of C_2F_6 into neutral fragments. The coefficients are generally better known than the cross sections although further measurements on electron diffusion coefficients and electron attachment at high E/N values are indicated. © *1998 American Institute of Physics and American Chemical Society.* [S0047-2689(98)00201-3]

Key words: C_2F_6, cross sections, electron attachment, electron collisions, electron transport, hexafluoroethane, ionization, perfluoroethane, scattering.

Contents

List of Tables

List of Figures

1. Introduction

In three earlier papers in this series we synthesized, evaluated, and extended the available information on electron collision processes with CF_4,[1] CHF_3,[2] and CCl_2F_2.[3] We have continued this effort to provide the most accurate information available on the electronic interactions of gases of interest to the semiconductor industry, and in this paper we report on perfluoroethane (C_2F_6, hexafluoroethane).

Perfluoroethane is a man-made gas with many applications. It is used in the aluminum industry, in the semiconductor industry, in plasma chemistry and etching applications,[4–9] in pulsed power switching gas mixtures,[10–20] and in carbon-13 separation.[21] It is of concern to the environment because it is a greenhouse gas with a very long residence time in the environment.[22] Its lifetime in the environment is reported[23,24] as 10 000 years and its global warming potential for a 100-year horizon[23] as 12 500, with reference to the global warming potential of CO_2 taken as equal to one (see also Maroulis *et al.*[25]). As is the case for other perfluorocarbon gases, it is difficult to remove C_2F_6 from the environment because of its extremely low decomposition rate and reactivity, although Morris *et al.*[26] have recently presented evidence that C_2F_6 is destroyed by reacting with O^+, and thus have identified an atmospheric loss mechanism for this gas.

As in our previous papers,[1–3] a number of collision cross sections, coefficients, and rate constants are used in this work to quantify various processes which result from the collisions of low-energy electrons with the C_2F_6 molecule. These are identified in Table 1 along with the corresponding symbols and units.

When possible, "recommended" cross sections and transport coefficients are given using the same criteria and procedure discussed in Christophorou *et al.*[1] As in the previous three papers of this series,[1–3] the recommended values are derived from fits to the most reliable data that are available at the time of preparation of this article and they are not necessarily "final." The recommended data are determined by the following criteria: (i) data are published in peer reviewed literature; (ii) no evidence of unaddressed errors; (iii) data are absolute determinations; (iv) multiple data sets are consistent with one another for overlapping ranges of electron

TABLE 1. Definition of symbols

Symbol	Definition	Common scale units
$\sigma_{ph}(\lambda)$	Photoabsorption cross section	10^{-18} cm^2; 10^{-22} m^2
$\sigma_{sc,t}(\varepsilon)$	Total electron scattering cross section	10^{-16} cm^2; 10^{-20} m^2
$\sigma_m(\varepsilon)$	Momentum transfer cross section (elastic)	10^{-16} cm^2; 10^{-20} m^2
$\sigma_{sc,el,d}(\varepsilon)$	Differential elastic electron scattering cross section	10^{-16} cm^2 sr^{-1}; 10^{-20} m^2 sr^{-1}
$\sigma_{sc,el}(\varepsilon)$	Integral elastic electron scattering cross section	10^{-16} cm^2; 10^{-20} m^2
$\sigma_{sc,in}(\varepsilon)$	Inelastic electron scattering cross section	10^{-16} cm^2; 10^{-20} m^2
$\sigma_{vib,d}(\varepsilon)$	Vibrational differential cross section	10^{-16} cm^2 sr^{-1}; 10^{-20} m^2 sr^{-1}
$\sigma_{vib,exc}(\varepsilon)$	Inelastic vibrational excitation cross section	10^{-16} cm^2; 10^{-20} m^2
$\sigma_{i,part}(\varepsilon)$	Partial ionization cross section	10^{-16} cm^2; 10^{-20} m^2
$\sigma_i(\varepsilon)$	Total ionization cross section	10^{-16} cm^2; 10^{-20} m^2
$\sigma_{diss}(\varepsilon)$	Total dissociation cross section	10^{-16} cm^2; 10^{-20} m^2
$\sigma_{diss,neut}(\varepsilon)$	Total cross section for dissociation into neutrals	10^{-16} cm^2; 10^{-20} m^2
$\sigma_a(\varepsilon)$	Total electron attachment cross section	10^{-16} cm^2; 10^{-20} m^2
α/N	Density-reduced ionization coefficient	10^{-22} m^2
$(\alpha - \eta)/N$	Effective ionization coefficient	10^{-22} m^2
$(E/N)_{lim}$	Limiting value of E/N	10^{-21} V m^2
η/N	Density-reduced electron attachment coefficient	10^{-22} m^2
$k_{a,t}$	Total electron attachment rate constant	10^{-10} cm^3 s^{-1}
$(k_{a,t})_{th}$	Thermal total electron attachment rate constant	$< 10^{-13}$ cm^3 s^{-1}
w	Electron drift velocity	10^6 cm s^{-1}
$(\mu N)_+$	Density-normalized thermal-electron mobility	10^{23} V^{-1} cm^{-1} s^{-1}
D_T/μ	Transverse electron diffusion coefficient to electron mobility ratio	V

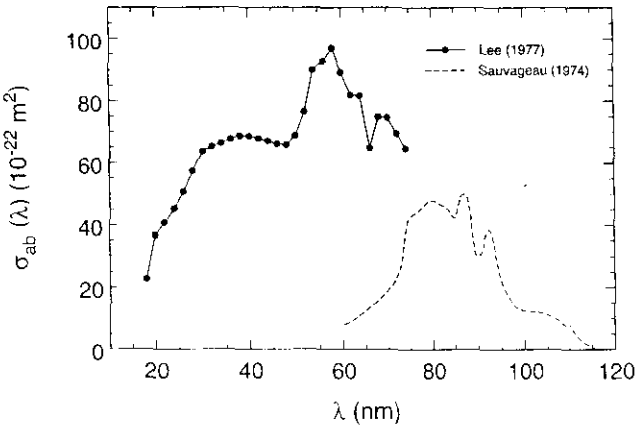

FIG. 1. Photoabsorption cross section, $\sigma_{ab}(\lambda)$, as a function of photon wavelength, λ, for C_2F_6; (---), Ref. 29; (●) Ref. 34.

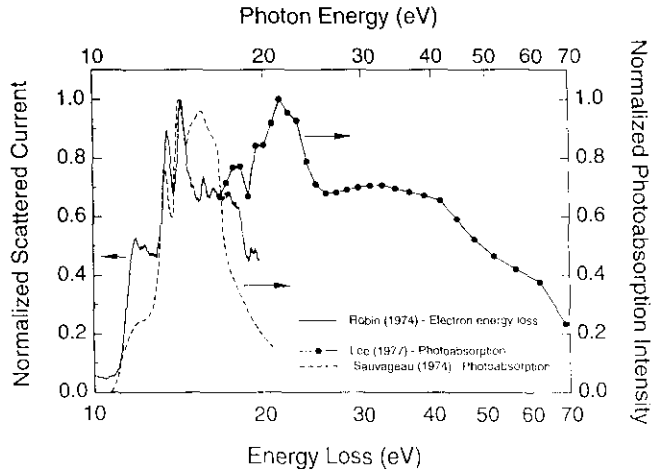

FIG. 2. Electron energy-loss spectrum (---) of C_2F_6 taken at a scattering angle $\theta=0°$ and at an incident electron energy of 100 eV (Ref. 30). For comparison the absoprtion data in Fig. 1 are also plotted as a function of photon energy (---), Ref. 29; (●), Ref. 34. The maximum intensity of each spectrum has been normalized to one.

energy within combined stated uncertainties; and (v) in regions where both experimentally and theoretically derived data exist, the experimental data are preferred. In instances where only a single set of data for a given cross section or coefficient satisfies the above-mentioned criteria, that set is designated as our recommended set and is tabulated as originally published. In cases where two or more data sets satisfy the selection criteria, each selected data set is analyzed by a weighted-least-squares (WLS) fit, with the resulting data having an equal spacing of points. This is done in order to ensure that each selected data set is equally weighted in the final fit regardless of the number of points in the original data. The recommended data set is then derived by a combined WLS fit to all of the data, and is presented in tabular and graphical format. When the above criteria are not satisfied, we either make no recommendation or "suggest" certain data in the absence of recommended values.

2. Electronic and Molecular Structure

The C_2F_6 molecule has D_{3d} symmetry. It has no permanent electric dipole moment[27] and has reported values[28] of static polarizability ranging from 46.0×10^{-25} cm^3 to 65.0×10^{-25} cm^3 depending on the method of calculation used. The absence of electron–electric dipole scattering has a rather profound effect on the electron scattering cross section at low energies (<1 eV) as compared to polar gases, which can be seen from the data presented later in the paper (Sec. 3).

Photoelectron spectra[29] of C_2F_6 show that the highest filled orbital in the ground state is mainly populated in the C–C bond, i.e., the uppermost molecular orbital (MO) is the C–C sigma σ_g MO.[29,30] Sauvageau *et al.*[29] interpreted the ultraviolet absorption spectrum of C_2F_6 in terms of Rydberg bands, some of which are superimposed on the ionization continuum. They ascribed the first ultraviolet (UV) band, observed at 12.10 eV, as a $3p$ type which is consistent with the assignment of Robin[30] who attributed the first allowed Rydberg excitation in C_2F_6 to the $\sigma_g\rightarrow3p$ transition at about 12.03 eV. The absorption spectrum of Sauvageau *et al.*[29] shows two sharp peaks at 13.40 eV ($\lambda=92.7$ nm; Fig. 1) and 14.25 eV ($\lambda=87$ nm; Fig. 1). The first ionization threshold energy has been found by Sauvageau *et al.*[29] to be at 14.6 eV and by Robin[30] at 14.48 eV. A mass spectrometric study of the photoionization of C_2F_6 conducted by Noutary[31] found no production of parent molecular ions. This study reported the energy thresholds for the photoionization processes

$$C_2F_6+h\nu\rightarrow C_2F_5^++F+e, \quad (1)$$

$$C_2F_6+h\nu\rightarrow CF_3^++CF_3+e, \quad (2)$$

to be (15.46±0.02) eV and (13.62±0.015) eV, respectively. The photoionization threshold for the production of the CF^+ ion was found to be 16.75 eV. These threshold values may not be adiabatic since the ions may have excess energy. A photoelectron–photoion coincidence spectrometric study by Simm *et al.*[32,33] showed that while the decomposition of ground state $C_2F_6^+$ ions gives entirely CF_3^+, and while the CF_3^+ ion is the predominant ion from highly excited states of $C_2F_6^+$, the $C_2F_6^+$ ions in their first excited state ($\tilde{A}$) decompose preferentially to $C_2F_5^++F$ prior to internally converting to the cationic ground state ($\tilde{X}$).

The photoabsorption cross section of C_2F_6 has been measured by Lee *et al.*[34] in the range 17.5–77.0 nm. The data of Lee *et al.* and those of Sauvageau *et al.*[29] are plotted in Fig. 1. The data of Sauvageau *et al.* are much lower and Lee *et al.* suggested that this difference may be due to the effect of stray light in the measurements of Sauvageau *et al.* An electron-impact energy-loss spectrum was published by Robin[30] and is reproduced in Fig. 2. Its shape is compared with the absorption spectra in Fig. 1 which have been replotted in Fig. 2 as a function of energy. All spectra were normalized to one at their maximum intensities to facilitate the comparison. There is substantial disagreement between the

TABLE 2. Photoabsorption cross section as a function of wavelength $\lambda, \sigma_{ab}(\lambda)$, for C_2F_6 [a]

Wavelength (nm)	Cross section (10^{-22} m^2)
18	22.7
20	36.7
22	40.8
24	45.2
26	50.7
28	57.5
30	63.7
32	65.3
34	66.5
36	67.7
38	68.8
40	68.7
42	68.0
44	67.2
46	66.3
48	66.0
50	69.0
52	76.6
54	90.0
56	92.8
58	97.0
60	89.2
62	82.0
64	81.8
66	65.0
68	75.0
70	74.7
72	69.5
74	64.8

[a]Data of Lee *et al.* (Ref. 34).

optical and the energy-loss measurements stressing the need for further measurements. The photoabsorption data of Lee *et al.* are listed in Table 2 since they are absolute cross section measurements over a broad energy range and since the data of Lee *et al.* for CF_4 (Ref. 1) and CHF_3 (Ref. 2) are generally in good agreement with other measurements for these molecules. However, more work is indicated both on photoabsorption and energy-loss spectra.

Absolute oscillator strength spectra in the C 1s (280–340 eV) and F 1s (680–740 eV) regions have been determined by Ishii *et al.*[35] from inner-shell electron energy-loss spectra using 2.5 keV energy electrons and scattering angles less than 2°. These investigators also measured the electron transmission spectrum of C_2F_6 and found negative ion resonances at 4.60 eV and 8.86 eV, which they attributed to σ^* molecular orbitals. These values are in reasonable agreement with electron attachment, electron scattering and vibrational excitation cross section data (see Table 3 and also Sec. 6 later in the paper).

Perfluoroethane is not a strong electron attaching gas. It, however, attaches electrons more efficiently than CF_4 and at relatively lower energies (see Sec. 6). No parent negative ion has been observed for perfluoroethane which is consistent with a negative electron affinity for this molecule.[35,36] The detection of $C_2F_6^-$ reported[37] recently in a study of C_2F_6 clusters is likely to be a metastable species associated with the lowest negative ion state of C_2F_6 at 4.0 eV. Clearly the data in Table 3 (Refs. 35, 36, 38–40; see also Sec. 6) show that there are at least two negative ion states at about 4 eV and 9 eV. Dissociative electron attachment studies indicate two other negative ion states at 4.8 eV and 12.5 eV; the latter may be due to an electron-excited Feshbach resonance. Electrons attach to C_2F_6 dissociatively mainly via the negative ion states at 4 eV and weakly via the negative ion states at 4.8 eV, 9 eV, and 12.5 eV. The predominant fragment negative ions are F^- and CF_3^- (see Sec. 6).

The energies of the 12 fundamental frequencies $\nu_1, \nu_2, \cdots \nu_{12}$ of C_2F_6 as listed by Shimanouchi[41] are: 0.1522 eV, 0.1001 eV, 0.0431 eV, 0.0084 eV, 0.1385 eV, 0.0885 eV, 0.1550 eV, 0.0767 eV, 0.0461 eV, 0.1551 eV, 0.0645 eV, and 0.0273 eV.

TABLE 3. Negative ion states of C_2F_6 [a]

Energy position (eV)	Type of study	Reference	Symmetry[a]
4.0[b]	Dissociative attachment producing F^- and CF_3^-	Table 19	$3a_{2u}(\sigma^*_{CC})$ Ref. 40
4.3	Vibrational excitation cross section function	Ref. 38	a_{2u} Ref. 38
4.6	Electron transmission	Ref. 35	
~5.0	Total electron scattering	Ref. 44	
4.8[c]	Dissociative attachment producing $C_2F_5^-$	Table 19, Sec. 6	$3a_{2u}(\sigma^*_{CF})$ Ref. 40
9.3	Maximum in the production of F	Ref. 39	
8.6	Maximum in the vibrational excitation cross section function	Ref. 38	e_u Ref. 38
8.86	Electron transmission	Ref. 35	
~9.0	Total electron scattering	Ref. 44	
12.5	Weak maximum in the production of F	Ref. 39	

[a]Ishii *et al.* (Ref. 35) calculated −3.73 eV, −4.24 eV, and −6.65 eV for the energies of the virtual orbitals e_u, a_{2u}, and a_{2u}. Lindholm and Li (Ref. 36) calculated the electron affinity of C_2F_6 to be −3.1 eV and the orbital to be σ^*C–C antibonding.

[b]Average position of the F^- and CF_3^- as determined in studies of dissociative attachment to C_2F_6 (see Table 19, Sec. 6).

[c]Average position of $C_2F_5^-$ as determined in studies of dissociative attachment to C_2F_6 (see Table 19, Sec. 6).

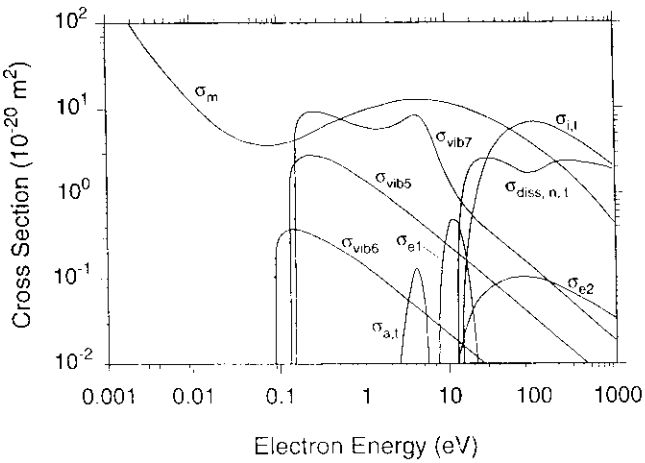

FIG. 3. A Boltzmann code analysis cross section set for electron collision processes with C_2F_6. The symbols σ_m, $\sigma_{i,t}$, $\sigma_{diss,n,t}$, σ_{e1}, σ_{e2}, $\sigma_{a,t}$, σ_{vib5}, σ_{vib6}, and σ_{vib7} refer, respectively, to the cross section for momentum transfer, total ionization, total dissociation into neutral fragments, excitation of the first electronic state, excitation of the second electronic state, total electron attachment, excitation of the v_5 vibration, excitation of the v_6 vibration, and excitation of the v_7 vibration (from Ref. 42). It should be noted, however, that σ_{e1} and σ_{e2} are arbitrary.

A set of electron-C_2F_6 collision cross sections has been derived by Hayashi and Niwa[42] from a Boltzmann code analysis (two term approximation). In their analysis Hayashi and Niwa used various cross sections from the literature as input, some of which they adjusted to optimize their final set of cross sections shown in Fig. 3. Their derived cross sections for individual processes and the ability of their cross-section set to generate transport coefficients can be seen from the comparisons in subsequent sections of the paper. A more recent cross section set for C_2F_6 has been obtained by Okumo and Nakamura[43] using multiterm Boltzmann analysis and new measurements of the electron drift velocity and the product of the longitudinal diffusion coefficient and gas number density they made in 0.524% and 5.4% C_2F_6–Ar, mixtures over the density reduced electric field range of 0.04×10^{-17}–100×10^{-17} V cm^2. The cross section set they reported[43] is similar to that of Hayashi and Niwa[42] except that the peak values of their σ_{vib6} and σ_{vib5} are larger, and the dip in their σ_{vib5} is more pronounced.

3. Electron Scattering

In this section information is presented and discussed on the following cross sections: total electron scattering cross section $\sigma_{sc,t}(\varepsilon)$, momentum transfer cross section (elastic) $\sigma_m(\varepsilon)$, differential elastic electron scattering cross section $\sigma_{e,diff}(\varepsilon)$, integral elastic electron scattering cross section $\sigma_{e,int}(\varepsilon)$, and inelastic electron scattering cross section $\sigma_{inel}(\varepsilon)$. The data are first presented in ways that facilitate their comparison and usefulness, and they are subsequently assessed and discussed. When possible, recommended cross section values are given.

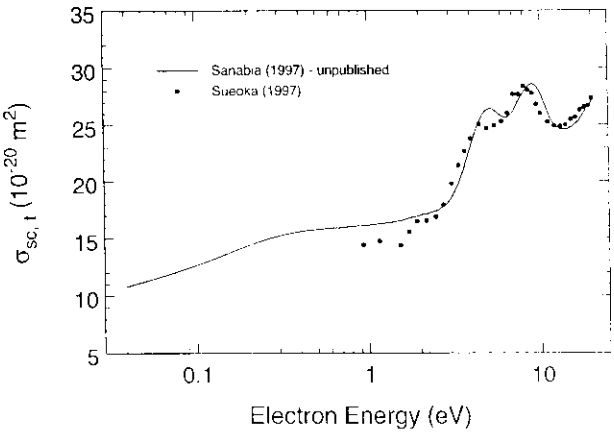

FIG. 4. Total electron scattering cross section, $\sigma_{sc,t}(\varepsilon)$, for C_2F_6: (—), Ref. 44; (●) Ref. 45.

3.1. Total electron scattering cross section, $\sigma_{sc,t}(\varepsilon)$

There have been two recent measurements[44,45] of $\sigma_{sc,t}(\varepsilon)$ for C_2F_6. These are presented in Fig. 4. They are in good agreement and the differences are well within the stated uncertainties of approximately ±20%. No calculated values of this cross section have been reported. The cross section of Sanabia *et al.*[44] has distinct structure with maxima at about 5.0 eV and 9.0 eV due to indirect electron scattering via the negative ion states located at these energies, which are also evident in the cross sections of Sueoka *et al.*[45] The cross section declines as the energy approaches zero due to the presence of a Ramsauer–Townsend minimum. However, due to the low-energy position of this minimum (see next section) the experiment of Sanabia *et al.* is unable to detect the low energy rise in $\sigma_{sc,t}(\varepsilon)$. Since the measurements of Sanabia *et al.*[44] were made over a wider energy range and with a better electron energy resolution than those of Sueoka *et al.*,[45] and since the two sets of data are in essential agreement, we have taken data points from the curve of Sanabia *et al.* in Fig. 4 as our suggested values for $\sigma_{sc,t}$. These are presented in Table 4.

3.2. Momentum transfer cross section (elastic), $\sigma_m(\varepsilon)$

There have been two calculations of the momentum transfer cross section (elastic) $\sigma_m(\varepsilon)$: one by Hayashi and Niwa[42] and the other by Pirgov and Stefanov.[46] These were both Boltzmann-type calculations based on measured values of the electron drift velocity, w, and transverse electron diffusion coefficient to mobility ratio, D_T/μ, as a function of E/N in the pure gas and in its mixtures with Ar. Pirgov and Stefanov used the w and D_T/μ data of Naidu and Prasad[47] and Hunter *et al.*[14] for pure C_2F_6, and the data of Hunter *et al.*[14] on w and D_T/μ for mixtures of C_2F_6 with Ar. They also used the measurements of Hunter *et al.*[14] for the dissociative electron attachment cross section of C_2F_6 and the data of Milloy *et al.*[48] and Spencer and Phelps[49] for the elastic momentum

TABLE 4. Suggested total electron scattering cross section, $\sigma_{sc,t}(\varepsilon)$ [a]

Electron energy (eV)	$\sigma_{sc,t}(\varepsilon)$ (10^{-20} m^2)
0.04	10.8
0.05	11.1
0.10	12.6
0.15	13.7
0.20	14.4
0.25	14.9
0.30	15.2
0.35	15.4
0.40	15.6
0.45	15.7
0.50	15.8
0.60	15.9
0.70	15.9
0.80	16.0
0.90	16.1
1.00	16.1
1.25	16.3
1.50	16.5
1.75	16.8
2.00	17.0
2.25	17.2
2.50	17.4
2.75	17.8
3.00	18.4
3.25	19.4
3.50	20.6
3.75	22.0
4.00	23.3
4.25	24.5
4.50	25.4
4.75	26.1
5.00	26.4
5.25	26.4
5.50	26.2
5.75	26.0
6.00	25.8
6.25	25.7
6.50	25.7
6.75	25.9
7.00	26.2
7.25	26.7
7.50	27.1
7.75	27.5
8.00	27.8
8.25	28.1
8.50	28.4
8.75	28.5
9.00	28.6
9.25	28.6
9.50	28.4
9.75	28.1
10.0	27.8
10.5	27.0
11.0	26.2
11.5	25.5
12.0	25.0
12.5	24.8
13.0	24.6
13.5	24.6
14.0	24.6
14.5	24.7
15.0	24.8
15.5	24.9
16.0	25.1
16.5	25.3
17.0	25.5
17.5	25.8
18.0	26.1
18.5	26.4
19.0	26.6
19.5	26.9
20.0	27.1

[a]From Ref. 44.

transfer cross section of argon. Hayashi and Niwa[42] used the same experimental data on w, D_T/μ, and electron attachment as Pirgov and Stefanov,[46] but in addition they employed input data for vibrational excitation, dissociation, and ionization (see Ref. 42). The results of these two studies are shown in Fig. 5. The two sets of calculations indicate a maximum in $\sigma_m(\varepsilon)$ at about 4 eV and a Ramsauer–Townsend minimum below 1 eV. The agreement between the results of the two calculations is rather poor both in regard to the magnitude and energy dependence of $\sigma_m(\varepsilon)$, and in regard to the position of the Ramsauer–Townsend minimum; ~0.08 eV for Ref. 42 and ~0.3 eV for Ref. 46.

There is only one published experimental determination of the $\sigma_m(\varepsilon)$ for C_2F_6 by Takagi *et al.*[38] which is also shown in Fig. 5. Takagi *et al.*[38] determined $\sigma_m(\varepsilon)$ by extrapolation and integration of their measurements on the absolute differential elastic scattering cross sections for C_2F_6. The latter measurements were made at electron energies of 2–100 eV and scattering angles of 10° to 130° and were extrapolated to 0° and 180°. The elastic momentum transfer cross sections were determined by numerical integration of the fits to the measured differential cross sections weighted by the factor $\sin\theta(1-\cos\theta)$. The uncertainty of these cross sections was quoted by the authors to be between 30% and 35%.

Recently, Dr. Merz[50] has provided us with a set of momentum transfer cross sections which were deduced from their currently unpublished measurements of the differential elastic scattering cross sections using a modified effective range theory (MERT)[51] analysis. These data are also shown in Fig. 5 and cover the low energy range between 0.01 eV and 6 eV. They show a pronounced Ramsauer–Townsend minimum at ~0.15 eV. The unpublished measurements of Merz and Linder[50] on the differential elastic scattering cross sections are in general agreement with those of Takagi *et al.*[38]

Compared to the two sets of experimental determinations[38,50] of $\sigma_m(\varepsilon)$, the results of the two Boltzmann-based computations[42,46] are in agreement with the measurements only near 3 eV.

In an effort to obtain values of $\sigma_m(\varepsilon)$ that can be suggested for possible use in modeling until more reliable direct measurements are made over a wider energy range, we performed a least-squares fit to the data of Merz and Linder[50] and those of Takagi *et al.*[38] to produce a cross section set that spans the complete range of energies. This suggested data set for $\sigma_m(\varepsilon)$ is shown in Fig. 5 by the bold solid line. Values obtained from this curve are listed in Table 5.

3.3. Differential elastic electron scattering cross section, $\sigma_{e,diff}(\varepsilon)$

Takagi *et al.*[38] reported measurements of the differential elastic electron scattering cross section, $\sigma_{e,diff}(\varepsilon)$, for C_2F_6 at electron-impact energies between 2 eV and 100 eV and scattering angles between 10° and 130°. These are given in Table 6 and are plotted in Fig. 6. The uncertainty in the values has been estimated by the authors to be between 15%

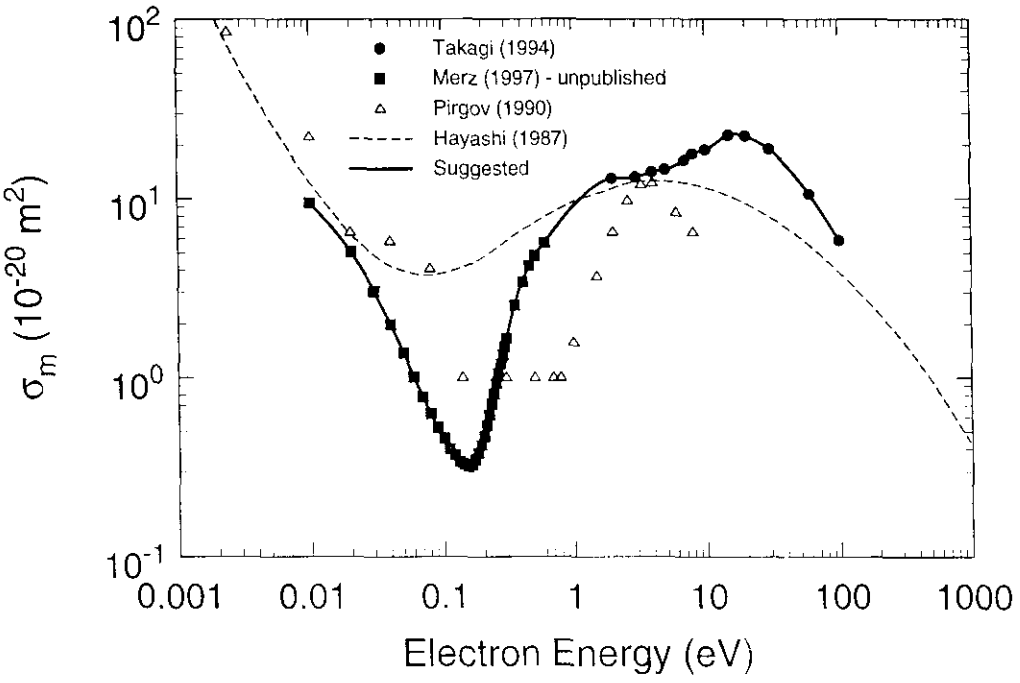

FIG. 5. Momentum transfer cross section (elastic), $\sigma_m(\varepsilon)$, for C_2F_6. Calculated values: (△) Ref. 46; (– –) Ref. 42. Measured: (●) Ref. 38. Deduced from differential scattering cross section measurements and MERT analysis: (■) Ref. 50. Suggested cross section: (——).

and 20%. The data were fitted under certain assumptions and extrapolated to 0° and 180° scattering angles (see Ref. 38). These fits are represented by the solid lines in the figure. They help provide data for scattering angles toward 0° and toward 180° which the authors used to determine the momentum transfer cross section (elastic) $\sigma_m(\varepsilon)$ discussed above, and the integral elastic electron scattering cross section $\sigma_{e,int}(\varepsilon)$ discussed below.

3.4. Integral elastic electron scattering cross section, $\sigma_{e,int}(\varepsilon)$

Takagi *et al.*[38] extrapolated their measured differential elastic electron scattering cross sections (Fig. 6) to 0° and 180° scattering angles, weighted them by sin θ, and obtained $\sigma_{e,int}(\varepsilon)$ by integration. Their values are given at the bottom of Table 6 and are plotted in Fig. 7. The quoted uncertainty is about 25%. To our knowledge there are no other published measurements or calculations of $\sigma_{e,int}(\varepsilon)$ for this molecule. However, we have recently been provided[50] with unpublished data on $\sigma_{e,int}(\varepsilon)$ which are also plotted in Fig. 7. These were deduced by Merz and Linder[50] from their unpublished measured differential elastic scattering cross sections using MERT and phase-shift analysis for energies below 0.5 eV and phase-shift analysis for energies above 0.5 eV. These data are in good agreement with the higher energy measurements of Takagi *et al.*[38] and extend the energy range of $\sigma_{e,int}(\varepsilon)$ down to 0.01 eV.

We fitted the two sets of data as shown by the bold solid line in Fig. 7, and values from this fit are listed in Table 7 as our presently suggested values for $\sigma_{e,int}(\varepsilon)$ of C_2F_6.

3.5. Inelastic electron scattering cross section, $\sigma_{inel}(\varepsilon)$

The only information on inelastic electron scattering processes in C_2F_6 is the work of Takagi *et al.*[38] on the vibrational excitation of this molecule. Takagi *et al.* studied the vibrational energy-loss spectra of C_2F_6 using various incident electron energies and scattering angles. Figure 8 shows the vibrational energy-loss spectra they obtained at incident electron energies of 2 eV, 4 eV, 7 eV and 8.5 eV and a scattering angle of 90°. In this figure, ν_s refers to excitation of a stretching mode and ν_b to a bending mode. The large energy-loss peak, ν_1, at 0.16 eV is mainly due to the excitation of the stretching vibrational mode, ν_1. The excitation spectrum of the ν_1 energy-loss stretching mode at 0.16 eV in the energy range 1.5–16.5 eV is shown in Fig. 9 for four scattering angles. At small scattering angles direct electron scattering is evident while at the larger scattering angles two distinct maxima are prominent at 4.3 eV and 8.5 eV which are attributed to shape resonances at these energies. Their relative intensity varies with scattering angle.[38]

The two Boltzmann code calculations[42,46] gave inelastic vibrational excitation cross sections as a function of electron energy which are shown in Fig. 10. Hayashi and Niwa[42] reported three such cross sections, σ_{vib5}, σ_{vib6}, and σ_{vib7}, while Pirgov and Stefanov[46] reported an overall inelastic vibrational cross section. We determined the sum of the three inelastic vibrational excitation cross sections of Hayashi and Niwa, which is shown in Fig. 10 by the solid line. It is in reasonable agreement with the overall cross section of Pirgov and Stefanov. For comparison the total scattering cross

TABLE 5. Suggested momentum transfer cross section, $\sigma_m(\varepsilon)$, for C_2F_6

Electron energy (eV)	$\sigma_m(\varepsilon)$ (10^{-20} m^2)
0.01	9.47
0.02	5.08
0.03	3.06
0.04	1.99
0.05	1.38
0.06	1.01
0.07	0.78
0.08	0.63
0.09	0.53
0.10	0.46
0.15	0.32
0.20	0.47
0.25	0.93
0.30	1.66
0.35	2.55
0.40	3.45
0.45	4.24
0.50	4.82
0.60	5.71
0.70	6.55
0.80	7.39
0.90	8.21
1.0	8.98
1.5	11.8
2.0	13.0
3.0	13.2
4.0	14.1
5.0	14.6
6.0	15.2
7.0	16.4
8.0	17.9
9.0	18.4
10.0	18.8
15.0	22.7
20.0	22.5
30.0	18.9
40.0	15.5
50.0	12.8
60.0	10.6
70.0	8.96
80.0	7.66
90.0	6.66
100	5.86

section, $\sigma_{sc,t}(\varepsilon)$, of Sanabia and Moore[44] is also plotted in Fig. 10.

Finally, it might be noted that a number of studies have indicated enhanced direct electron scattering from vibrationally excited C_2F_6 molecules.[52–54] It is possible that this enhancement is due to the dipole moments that some of the excited vibrational modes may induce.

4. Electron-Impact Ionization

4.1. Partial ionization cross section, $\sigma_{i,part}(\varepsilon)$

Poll and Meichsner[55] measured the partial ionization cross sections for CF^+, CF_2^+, CF_3^+, and $C_2F_5^+$ produced by electron impact on C_2F_6 in the energy range of about 12.8 V to about 130 eV. The CF_3^+ ion has the largest cross section of all four fragment ions. We digitized their data from the graphs presented in their paper[55] in order to obtain the values listed in Table 8 and plotted in Fig. 11. The broken portions of the curves in the figure indicate data which could not be determined accurately from the linear plots of Poll and Meichsner. Clearly there seems to be a problem with these data at low energies. The partial ionization cross section for CF_3^+ (and possibly $C_2F_5^+$) as determined from the figure of Poll and Meichsner has finite values below the accepted values of the appearance potentials (A.P.) for these ions (see Table 9 discussed below). These "long tails" were noted by Poll and Meichsner who advanced two possible reasons for them: ionization of vibrationally excited molecules and/or the effect of the broad ("some eV") electron energy distribution in their experiments. The latter cause seems most likely. This uncertainty is the largest for the most abundant ion, CF_3^+, but it is unclear why a similar effect is not observed for the less abundant ions, CF^+ and CF_2^+.

The available data on appearance potentials for ions from C_2F_6 are presented in Table 9. The appearance potentials for the four fragment cations, CF_3^+, $C_2F_5^+$, CF^+, and CF_2^+ are derived from the available electron-impact data presented in Table 9, and are indicated in Fig. 11. They are, respectively, 16.0 eV (average of the two electron impact values), 15.8 eV (average of the two electron impact values), 18.0 eV, and 17.5 eV.

The only other measurement of the partial ionization cross sections for C_2F_6 is that of Bibby and Carter[56] for only one value of incident electron energy. Bibby and Carter reported the following cross section values at 35 eV: 0.22×10^{-17} cm^2 for CF^+, 3.16×10^{-17} cm^2 for CF_3^+, and 2.57×10^{-17} cm^2 for $C_2F_5^+$; which all fall nearly an order of magnitude below the corresponding values of Poll and Meichsner.[55] The sum of these partial ionization cross sections at 35 eV is 5.95×10^{-17} cm^2 which is about 7.4 times smaller than the corresponding value from Ref. 55 (discussed in the next section).

4.2. Total ionization cross section, $\sigma_{i,t}(\varepsilon)$

There have been four measurements of the total ionization cross section $\sigma_{i,t}(\varepsilon)$ of the C_2F_6 molecule. The first was made by Kurepa[57] for incident electron energies up to 100 eV. No uncertainty was assigned to these measurements. They are plotted in Fig. 12 as open squares. At energies above ~60 eV they diverge considerably from the more recently obtained data. The second measurement of $\sigma_{i,t}(\varepsilon)$ was made by Beran and Kevan[58] for only three values of incident electron energy. These results are shown in Fig. 12 by the × symbols. However, the data of Beran and Kevan[58] for a number of other molecular species are consistently higher than those of Rapp and Englander-Golden[59] which are generally accepted to be more accurate. The ratio of the $\sigma_{i,t}(\varepsilon)$ values as measured by Rapp and Englander-Golden to those measured by Beran and Kevan at 35 eV and 70 eV for a number of species is 0.85. We thus have multiplied the original cross section values of Beran and Kevan[58] by this factor and the so adjusted cross sections are shown in Fig. 12 by the open

TABLE 6. Differential elastic electron scattering cross section, $\sigma_{e,\mathrm{diff}}(\varepsilon)$, for C_2F_6 in units of 10^{-20} m^2 sr^{-1}. At the bottom of the table are given the values of $\sigma_{e,\mathrm{int}}(\varepsilon)$ and $\sigma_m(\varepsilon)$ as determined from these measurements[a]

Deg.	2 eV	3 eV	4 eV	5 eV	7 eV	8 eV	10 eV	15 eV	20 eV	30 eV	60 eV	100 eV
10										23.54	41.13	37.91
15					5.30	7.05	8.26	11.28	15.45		19.31	11.26
20	0.46	1.04	2.11	3.96	5.54	6.88	7.80	8.70	10.09	14.07	6.47	2.77
25											2.09	1.86
30	0.93	1.76	2.56	4.27	5.33	5.77	5.68	5.33	4.13	3.22	1.37	1.61
40	1.37	2.50	2.81	4.09	4.13	4.09	3.32	2.27	1.17	1.15	1.43	0.86
50	1.84	2.77	2.66	3.37	2.80	2.37	1.49	1.15	1.02	1.69	0.95	0.40
60	1.95	2.44	2.16	2.19	1.55	1.23	0.95	1.23	1.48	1.68	0.58	0.36
70	1.96	2.02	1.65	1.47	0.94	0.88	1.03	1.63	1.60	1.24	0.41	0.31
80	1.84	1.59	1.11	1.19	0.84	0.94	1.24	1.81	1.41	0.86	0.24	0.19
90	1.39	1.17	0.98	1.06	1.06	1.11	1.33	1.55	1.17	0.76	0.21	0.16
100	1.13	0.89	0.83	0.95	1.05	1.13	1.19	1.37	0.96	0.51	0.24	0.14
110	1.07	0.82	0.78	0.89	0.93	0.93	1.03	1.11	0.80	0.54	0.29	0.17
120	0.81	0.69	0.67	0.82	0.76	0.83	1.01	1.12	0.90	0.78	0.45	0.25
130	0.72	0.72	0.60	0.63	0.77	0.90	0.85	1.21	1.23	1.15	0.59	0.34
$\sigma_{e,\mathrm{int}}$	15.53	17.61	19.11	21.19	22.66	24.26	24.88	28.04	28.09	25.33	21.51	16.12
σ_m	12.98	13.18	14.11	14.56	16.43	17.85	18.81	22.73	22.45	18.93	10.62	5.86

[a]See the text and Ref. 38.

circles. The third set of values are those obtained by summation of the partial ionization cross sections measured by Poll and Meichsner[55] (last column of Table 8) as discussed in the last section. These are shown in Fig. 12 by the long dashed line. The fourth measurement, as mentioned in the preceding section, is an early report[56] of a measurement of the ionization cross section for the production of the CF^+, CF_3^+ and $C_2F_5^+$ ions from C_2F_6 at one value of the electron energy,

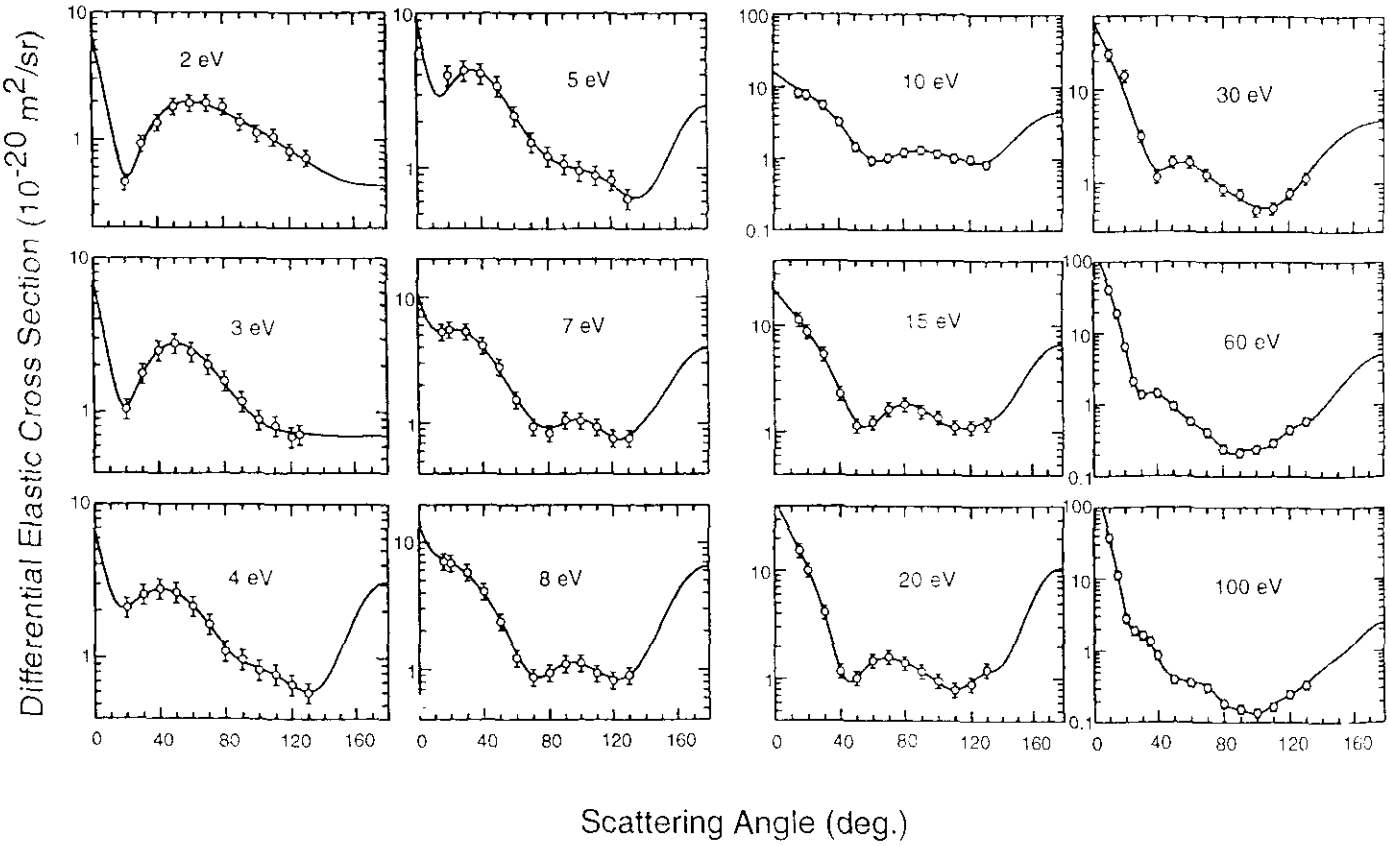

FIG. 6. Differential elastic electron scattering cross sections, $\sigma_{e,\mathrm{diff}}(\varepsilon)$, for C_2F_6 (from Ref. 38).

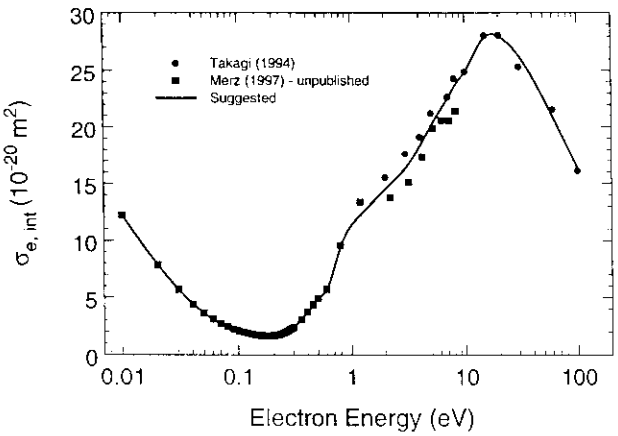

FIG. 7. Integral elastic electron scattering cross section, $\sigma_{e,int}(\varepsilon)$ for C_2F_6. (●) Ref. 38; (■), Ref. 50; (—), suggested cross section.

namely 35 eV. At this electron energy the sum of the cross section of Bibby and Carter[56] for the three ions is equal to 0.6×10^{-20} m^2. It is shown in Fig. 12 by the solid circle, and is obviously well below the other experimental data.

Finally, Fig. 12 shows the cross section deduced from a Boltzmann code analysis by Hayashi and Niwa,[42] and the cross section calculated recently by Kim[60] using a model[61] that combines binary encounter theory and the Bethe theory of electron impact ionization. The calculated cross sections are in reasonable agreement with the measurements, although the Hayashi and Niwa cross section lies well below the measurements at high energies [see Fig. 12(a)] and the Kim cross section lies below the measurements at low energies [see Fig. 12(b).]

It is difficult to recommend values for the $\sigma_{i,t}(\varepsilon)$ of C_2F_6 especially in view of the uncertainty in the measurements of Poll and Meichsner at electron energies approaching the ionization thresholds. However, we suggest the following as a reasonable attempt. Accept a value of 15.9 eV for the ionization threshold of C_2F_6 (based upon the ionization thresholds in Table 9 for CF_3^+ and $C_2F_5^+$) and assume that $\sigma_{i,t}(\varepsilon)$ is zero at this energy. Average the cross section values of Poll and Meichsner and the adjusted cross section values of Beran and Kevan at the three energies (20 eV, 35 eV, and 70 eV) at which data from both sources exist. Then fit a curve to these three average cross section values and a zero value at 15.9 eV. This fitting is shown in the Fig. 12 by the solid heavy line. Cross section values taken off this curve are listed in Table 10 as our suggested cross section $\sigma_{i,t}(\varepsilon)$ for C_2F_6.

4.3. Total dissociation cross section, $\sigma_{diss,t}(\varepsilon)$

The only measurement of the total dissociation cross section we know of is that by Winters and Inokuti.[62] This cross section is presented in Fig. 13 and in Table 11, and represents the sum of the cross sections for dissociative ionization and the cross sections for electron impact dissociation into neutral fragments with a reported uncertainty of ±20%. An estimate may be obtained of the total cross section for dissociation into neutral species, $\sigma_{diss,neut,t}(\varepsilon)$ by subtracting the total ionization cross section $\sigma_{i,t}(\varepsilon)$, which is exclusively due to dissociative ionization, from the total dissociation cross section of Winters and Inokuti. This difference is shown in Fig. 13 by the closed triangles. These values must be considered a gross estimate due to the previously discussed uncertainties in the values suggested for $\sigma_{i,t}(\varepsilon)$ and the relatively large stated uncertainty of $\sigma_{diss,t}(\varepsilon)$. They seem to be consistent with the values of $\sigma_{diss,neut,t}(\varepsilon)$ deduced by Hayashi and Niwa.[42] Preliminary measurements by Motlagh and Moore[63] of the cross section for the production of CF_3 radicals by electron impact on C_2F_6 are also qualitatively consistent with these cross sections for neutral dissociation in that they also observe a peak near 22 eV. Motlagh and Moore measured the production of CF_3 radicals due to electron impact on C_2F_6 by detecting volatile $Te(CF_3)_2$ molecules resulting from the reaction of CF_3 radicals with solid

TABLE 7. Suggested integral elastic electron scattering cross section, $\sigma_{e,int}(\varepsilon)$, for C_2F_6

Electron energy (eV)	$\sigma_{e,int}(\varepsilon)$ (10^{-20} m^2)
0.01	12.23
0.02	7.86
0.03	5.68
0.04	4.41
0.05	3.61
0.06	3.07
0.07	2.70
0.08	2.43
0.09	2.23
0.10	2.07
0.15	1.69
0.20	1.66
0.25	1.91
0.30	2.39
0.40	3.70
0.50	4.91
0.60	5.71
0.70	7.54
0.80	9.39
0.90	10.6
1.0	11.3
1.5	13.2
2.0	14.5
3.0	16.3
4.0	18.3
5.0	20.1
6.0	21.4
7.0	22.5
8.0	23.5
9.0	24.3
10.0	24.9
15.0	27.9
20.0	28.0
30.0	26.3
40.0	24.4
50.0	22.5
60.0	20.9
70.0	19.6
80.0	18.4
90.0	17.3
100	16.4

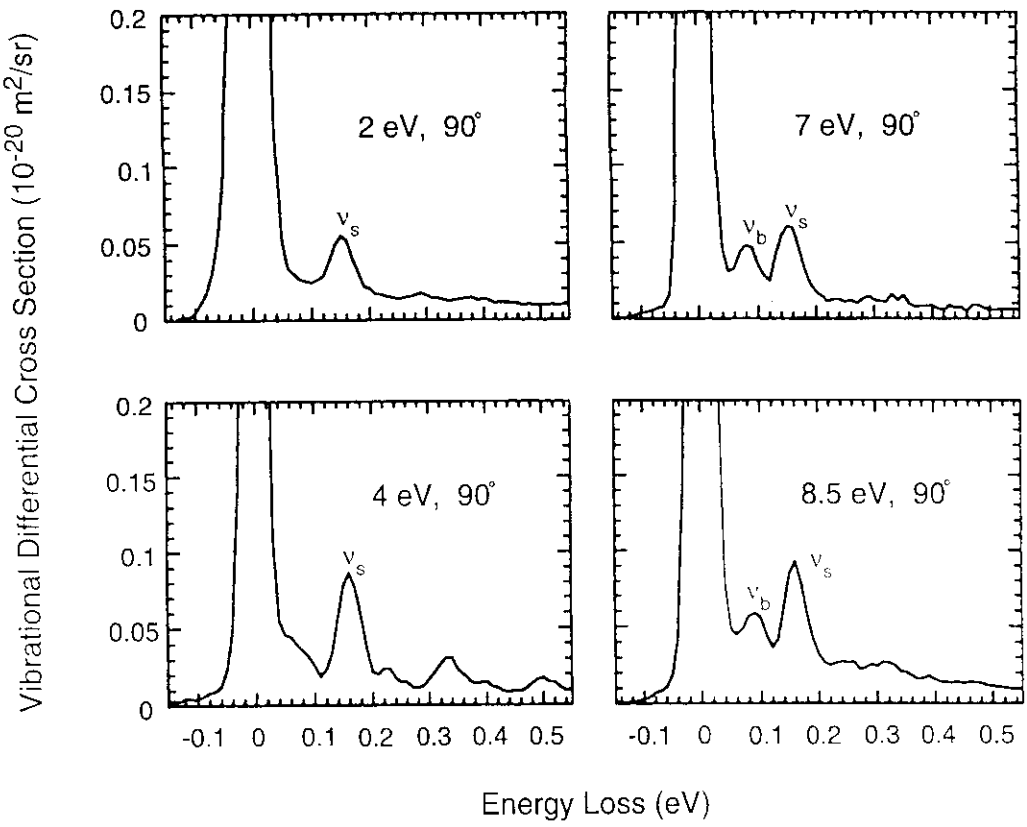

FIG. 8. Vibrational differential cross section, $\sigma_{\text{vib, diff}}(\varepsilon)$, as a function of electron energy for various vibrational energy losses at a scattering angle of 90° and incident electron energies of 2 eV, 4 eV, 7 eV, and 8.5 eV. The symbol ν_s refers to a stretching and ν_b to a bending mode. The ν_s peak consists mainly of the vibrational mode ν_1 (from Ref. 38).

tellurium. The magnitude of their cross section is below the values discussed above by approximately a factor of 3.

4.4. Ionization coefficients

4.4.1. Density-reduced ionization coefficient, α/N

The density-reduced ionization coefficient α/N is measured as a function of electric field-to-gas density ratio E/N. It is related to the normalized electron-energy distribution function $f(\varepsilon, E/N)$ and the total ionization cross section $\sigma_{i,t}(\varepsilon)$ by

$$\alpha/N(E/N) = (2/m)^{1/2} w^{-1} \int_I^\infty f(\varepsilon, E/N) \varepsilon^{1/2} \sigma_{i,t}(\varepsilon) d\varepsilon, \qquad (3)$$

where I is the ionization threshold energy of the C_2F_6 molecule (see Table 9) and m is the electron mass. There have been a number of measurements[47,64–66] of α/N as a function of E/N for C_2F_6 at temperatures ranging from 293 K to 298 K. These measurements were performed at pressures below about 13 kPa and the authors generally quoted uncertainties of ±10%, with the exception of Naidu and Prasad[47] who reported an overall uncertainty between ±10% for E/N values lower than the limiting value of E/N (see Sec. 4.4.3.) and ±20% for higher values of E/N. All measurements were made using the steady-state Townsend method, except those of Hunter *et al.*[65] who used a pulsed-Townsend method. These measurements are compared in Fig. 14. The ionization coefficient is not expected to be sensitive to small variations in gas temperature and indeed the measurements of Hunter *et al.*[65] found no noticeable change in the values of α/N at 300 K and at 500 K.

The data between 210×10^{-21} V m^2 and 400×10^{-21} V m^2 in Fig. 14 (the range in which all the data overlap) were least-squares fitted and their average is shown in the figure by the solid line. Below 210×10^{-21} V m^2 the data of Hunter *et al.* were normalized to the average value at 210×10^{-21} V m^2. Above 400×10^{-21} V m^2, the data of Naidu and Prasad were normalized to the mean value at 400×10^{-21} V m^2. The resultant values are shown in Fig. 14 by the solid line and are listed in Table 12 as our recommended data for the density-normalized ionization coefficient α/N of C_2F_6. The broken lines in Fig. 14 are the calculated values of Hayashi and Niwa,[42] which are in reasonable agreement with the recommended data.

As far as we know there have been no reported measurements of α/N for C_2F_6 in gas mixtures.

4.4.2. Effective ionization coefficient, $(\alpha-\eta)/N$

Figure 15 shows the values of the effective ionization coefficient $(\alpha-\eta)/N(=\bar{\alpha}/N)$ for C_2F_6 as a function of E/N measured by various groups at two temperatures; ~300 K and 500 K. The room temperature data are those of Carter

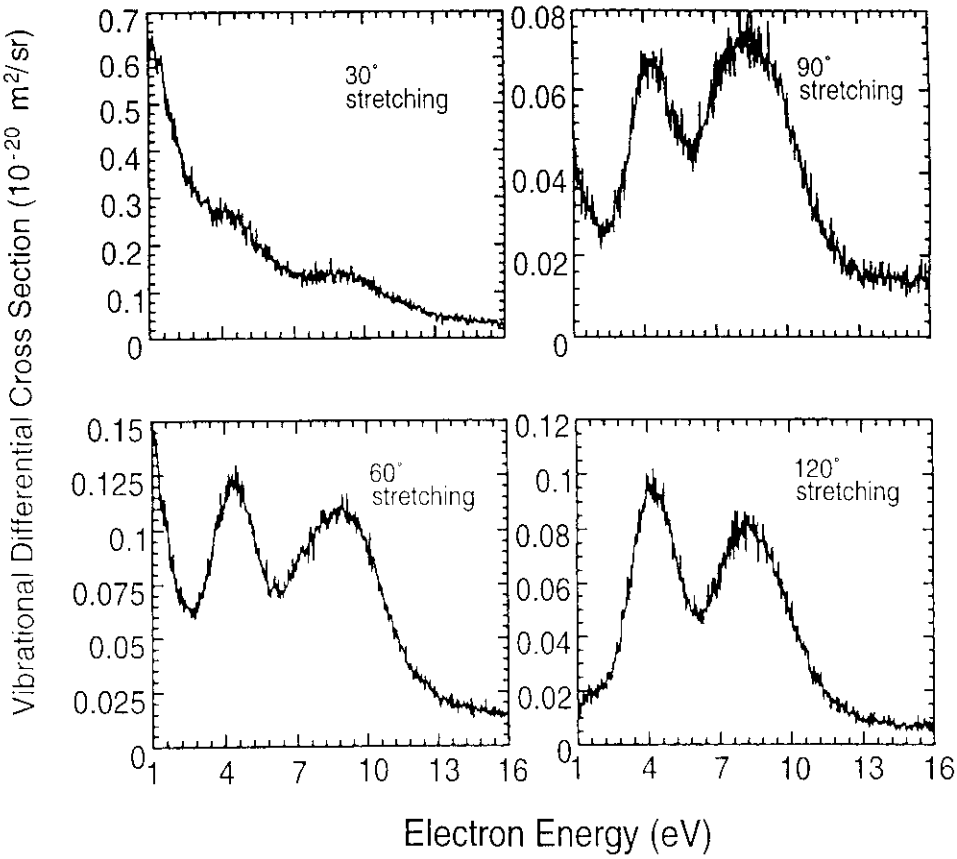

FIG. 9. Excitation functions for the vibrational energy-loss peak v_s(0.16eV) at the indicated scattering angles (from Ref. 38).

et al.,[67] Hunter *et al.*,[65] Naidu and Prasad,[47] and Božin and Goodyear.[66] The only data at a temperature other than ambient are those of Carter *et al.*[67] at 500 K. The reported uncertainties are all about ±10 %, except for Hunter *et al.* (~5 %) and Naidu and Prasad (between 10% and 20% at high E/N).

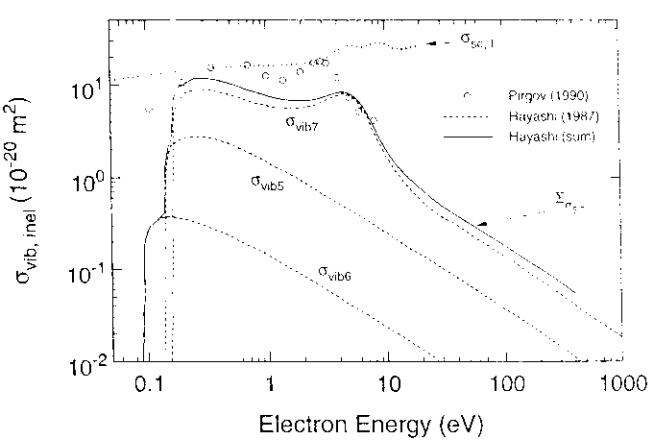

FIG. 10. Inelastic vibrational excitation cross section as a function of electron energy, $\sigma_{vib,inel}(\varepsilon)$, for C_2F_6. (---) calculated cross sections for three vibrational modes (Hayashi and Niwa, Ref. 42); (—), sum of the three cross sections of Hayashi and Niwa; (○) overall inelastic vibrational excitation cross section calculated by Pirgov and Stefanov, (Ref. 46); (...) $\sigma_{sc,1}$ from Ref. 44.

Interestingly, the values of $(\alpha-\eta)/N$ at 500 K are lower than at 300 K although at these two temperatures the values of α/N are virtually the same. Clearly the temperature dependence of $(\alpha-\eta)/N$ is due to the temperature dependence of the electron attachment coefficient η/N (see Sec. 6.1.).

A least-squares fit to the room-temperature data is represented in Fig. 15 by the solid line. Points taken off this curve are listed in Table 13 as our recommended values for the $(\alpha-\eta)/N$ of C_2F_6.

It is finally noted that Byszewski *et al.* reported effective ionization rates for pure C_2F_6,[68,69] and for mixtures of C_2F_6 in Ar.[69]

4.4.3. $(E/N)_{lim}$

The limiting value of electric field-to-gas density ratio, $(E/N)_{lim}$, is the value of E/N at which $(\alpha-\eta)/N=0$. It comes naturally from the values of the electron-impact ionization and electron attachment coefficients measured as functions of E/N. The $(E/N)_{lim}$ value should coincide with the breakdown voltage of C_2F_6 as measured under a uniform electric field. In Table 14 are listed values of $(E/N)_{lim}$ measured at room temperature. Their average is 275×10^{-21} V m^2. Interestingly, Christophorou *et al.*[70,71] found that $(E/N)_{lim}$ increases with increasing temperature (see Table 14) and this increase has been attributed to an increase in the dissociative electron attachment cross section with increasing temperature for this molecule (see Sec 6.6.

TABLE 8. Partial ionization cross sections, $\sigma_{i,\,part}(\varepsilon)$, for C_2F_6 in units of 10^{-20} m^2 [a]

Electron energy (eV)	$\sigma_{i,\,part}(\varepsilon)$ CF_3^+	$\sigma_{i,\,part}(\varepsilon)$ $C_2F_5^+$	$\sigma_{i,\,part}(\varepsilon)$ CF^+	$\sigma_{i,\,part}(\varepsilon)$ CF_2^+	$\sigma_{i,\,t}(\varepsilon)$ Sum
13.0	(0.03)[b]	...	...	...	(0.03)
14.0	(0.08)	...	...	...	(0.08)
15.0	0.14	...	...	...	0.14
16.0	0.20	(0.07)	...	...	0.27
17.0	0.27	0.15	...	...	0.42
18.0	0.35	0.23	...	...	0.57
19.0	0.43	0.30	...	...	0.73
20.0	0.52	0.39	(0.02)	...	0.93
22.0	0.73	0.60	(0.04)	...	1.37
24.0	0.96	0.79	0.07	(0.02)	1.83
26.0	1.20	0.96	0.09	0.03	2.27
28.0	1.47	1.15	0.11	0.04	2.77
30.0	1.74	1.31	0.14	0.06	3.26
35.0	2.34	1.69	0.23	0.11	4.38
40.0	2.83	2.02	0.33	0.18	5.36
45.0	3.20	2.28	0.44	0.24	6.16
50.0	3.46	2.43	0.52	0.30	6.71
55.0	3.64	2.54	0.60	0.34	7.12
60.0	3.76	2.60	0.67	0.38	7.41
65.0	3.85	2.63	0.71	0.40	7.59
70.0	3.90	2.65	0.75	0.42	7.72
75.0	3.93	2.66	0.78	0.43	7.81
80.0	3.95	2.66	0.81	0.44	7.86
85.0	3.97	2.65	0.83	0.45	7.90
90.0	3.98	2.64	0.84	0.45	7.91
95.0	3.98	2.62	0.86	0.46	7.93
100.0	3.98	2.60	0.87	0.46	7.91
105.0	3.98	2.58	0.88	0.46	7.91
110.0	3.98	2.55	0.90	0.46	7.89
115.0	3.96	2.52	0.91	0.46	7.86
120.0	3.95	2.49	0.92	0.46	7.82
125.0	3.93	2.45	0.93	0.46	7.77

[a]Data from Ref. 55.
[b]Values in parentheses could not be accurately determined from the graphs of Ref. 55.

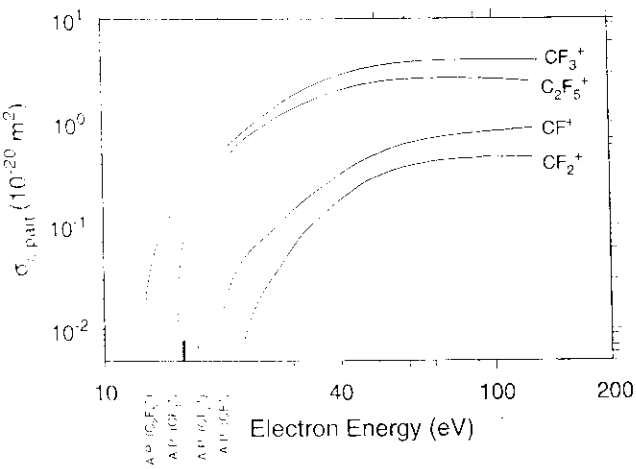

FIG. 11. Partial electron-impact ionization cross sections $\sigma_{i,\,part}(\varepsilon)$ as a function of electron energy for C_2F_6 (from Ref. 55). The broken curves indicate that the cross section values could not be determined accurately from the plots of Poll and Meichsner. The appearance potentials (as determined from the values in Table 9) for the four fragment ions are also shown in the figure.

TABLE 9. Appearance potentials or ionization threshold energies[a] for C_2F_6

Energy (eV)	Method and reference
14.6	Photoabsorption spectra Ref. 29
14.48 (vertical)	Photoelectron spectra Ref. 30
13.62±0.015 (CF_3^+) 15.46±0.02 ($C_2F_5^+$) 16.75 (CF^+)	Photoionization Ref. 31
15.4 (CF_3^+) 16.05 ($C_2F_5^+$) 22.6 (F^+)	Electron impact Ref. 56
16.5 (CF_3^+) 15.5 ($C_2F_5^+$) 17.5 (CF_2^+) 18.0 (CF^+)	Electron impact Ref. 55

[a]The photoionization threshold energies are lower than the corresponding electron impact threshold energies. This reflects the large differences between the energies of the vertical and the adiabatic transitions leading to dissociative ionization for this molecule.

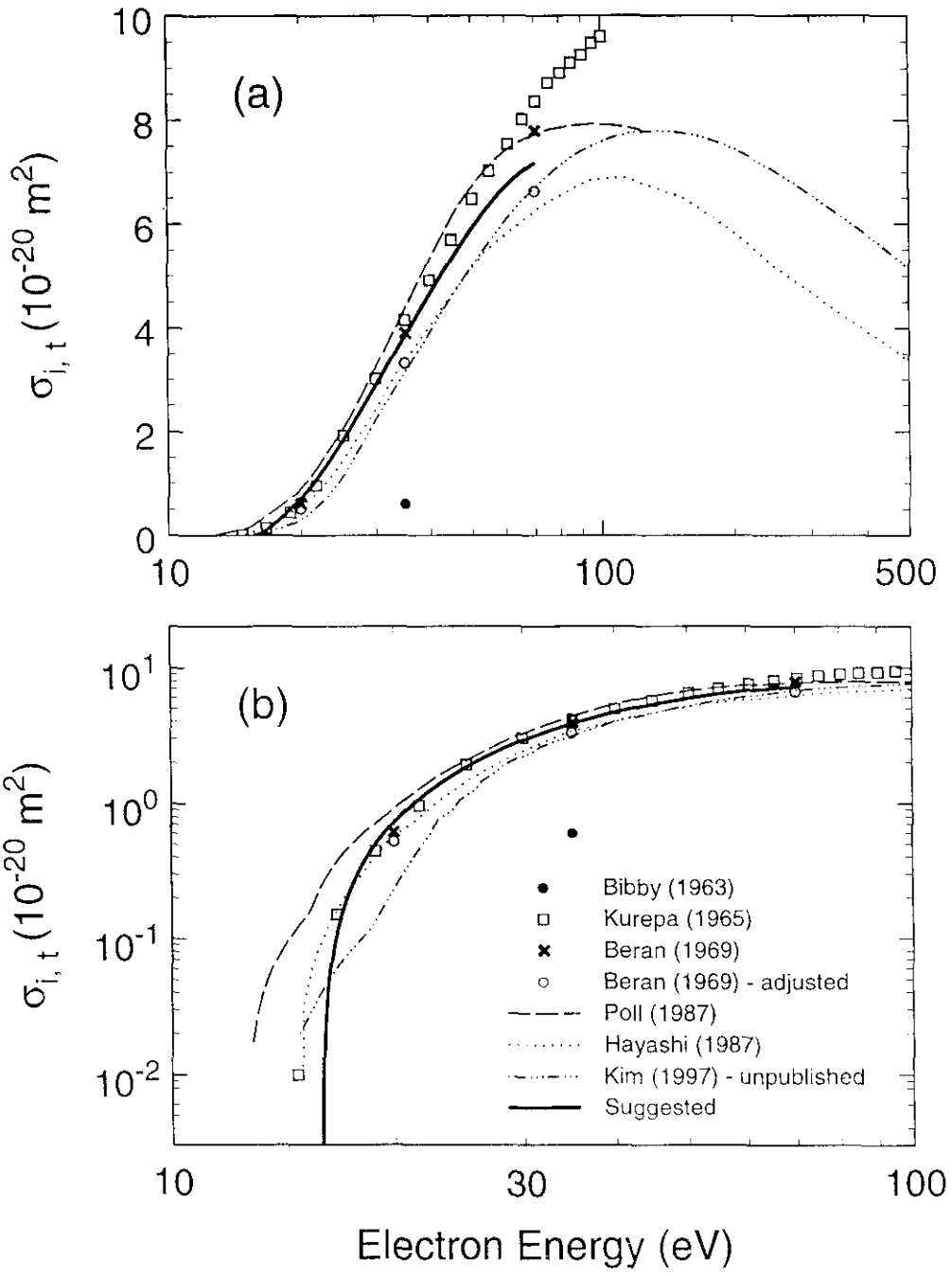

FIG. 12. Total ionization cross section as a function of electron energy, $\sigma_{i,t}(\varepsilon)$, for C_2F_6. (a) Semilog plot illustrating the uncertainties at high energies; (b) Log-log plot illustrating the uncertainties at low energies; (●) Ref. 56; (□) Ref. 57; (×) Ref. 58; (○) Ref. 58 adjusted; (– –), Ref. 55 (sum of partial ionization cross sections, last column in Table 8); (...) Ref. 42; (–...–) Ref. 60; (—), suggested cross section.

and Refs. 70 and 71). The least-squares fits to the data in Fig. 15 for 300 K and 500 K gave values of $(E/N)_{\lim}$ equal to 273×10^{-21} V m^2 at 300 K and 291×10^{-21} V m^2 at 500 K.

Furthermore, measurements have been made of the $(E/N)_{\lim}$ of binary mixtures of C_2F_6 with Ar or CH_4 for pulse power applications.[12] Figure 16 shows these measurements.

4.4.4. Average energy to produce an electron–ion pair, *W*

The average energy to produce an electron–ion pair, W, for α particles (initial energy ~5.1 MeV) has been measured by Nakanishi *et al.*[77] for pure C_2F_6 and found to be 34.7 eV per ion pair. A similar measurement by Reinking *et al.*[78] gave a value of 34.5 eV per ion pair. These values are almost identical with those measured by Reinking *et al.*[78] for CF_4 and C_3F_8. They are large compared to the W values of other polyatomic molecules,[79] reflecting the high ionization threshold energies for these perfluorocarbon molecules and the considerable amount of energy going into translational and/or internal energy of the fragments that accompany the dissociative ionization processes in these molecules. Nagra and Armstrong[80] measured the W of C_2F_6 using ^{60}Co γ rays and found it to be 32.7 eV per ion pair. This value is lower than that for α particles, as expected.[79]

TABLE 10. Suggested total ionization cross section, $\sigma_{i,t}(\varepsilon)$, for C_2F_6

Electron energy (eV)	$\sigma_{i,t}(\varepsilon)$ (10^{-20} V m^2)
16.0	0.015
18.0	0.33
20.0	0.72
22.0	1.15
25.0	1.82
30.0	2.89
35.0	3.84
40.0	4.66
45.0	5.34
50.0	5.91
55.0	6.36
60.0	6.71
65.0	6.98
70.0	7.17

Nakanishi *et al.*[77] and Reinking *et al.*[78] measured the W values for binary mixtures of C_2F_6 with Ar and C_2H_2. Figure 17 shows these measurements. Nakanishi *et al.*[77] also made measurements of W for binary mixtures of C_2F_6 with 2-C_4H_8.

5. Electron Impact Dissociation Producing Neutrals

To our knowledge there are no data on this important process, except the estimates discussed in Sec. 4.3., and the recent preliminary, unpublished measurements of Motlagh and Moore[63] discussed in Sec. 4.3. It might be of interest to note that measurements of neutral fragments in various low pressure C_2F_6 discharges have been made[81,82] using diode laser absorption spectroscopy.

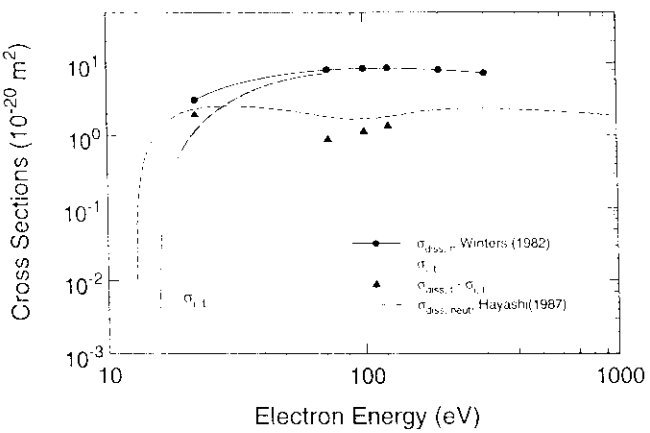

FIG. 13. Total dissociation cross section as a function of electron energy, $\sigma_{diss,t}(\varepsilon)$, for C_2F_6. (—●—), data of Winters and Inokuti (Ref. 62). Also plotted in the figure are the suggested total ionization cross section $\sigma_{i,t}(\varepsilon)$ [(– – –) from Table 10] and the difference between the two, $\sigma_{diss,t}(\varepsilon) - \sigma_{i,t}(\varepsilon)$. The short dashed curve (---) is the calculated $\sigma_{diss,neut,t}(\varepsilon)$ of Hayashi and Niwa (Ref. 42).

TABLE 11. Total dissociation cross section, $\sigma_{diss,t}(\varepsilon)$ for C_2F_6[a]

Electron energy (eV)	$\sigma_{diss,t}(\varepsilon)$ (10^{-20} m^2)
22	3.1
72	8.1
100	8.5
125	8.6
200	8.1
300	7.3

[a]Reference 62.

6. Electron Attachment

There have been a number of measurements of electron attachment coefficients in C_2F_6. We begin this section by analyzing these measurements first because they provide insight into understanding the electron attachment cross section data which are presented later in this section. These data are also useful in many practical applications and in computations aimed at deriving cross section sets for this molecule.

6.1. Density-reduced electron attachment coefficient, η/N

The density-reduced electron attachment coefficient, η/N, of C_2F_6 has been measured as a function of E/N both in the pure gas and in mixtures of C_2F_6 with a number of buffer gases. The quantity $\eta/N(E/N)$ is related to the total electron attachment cross section, $\sigma_{a,t}(\varepsilon)$, and the electron energy distribution function $f(\varepsilon,E/N)$ in the gas or gas mixture by

$$\eta/N_a(E/N) = (2/m)^{1/2} w^{-1} \int_0^\infty f(\varepsilon,E/N)\varepsilon^{1/2}\sigma_{a,t}(\varepsilon)d\varepsilon, \tag{4}$$

where N_a is the number density of the electron attaching gas and w is the electron drift velocity. For the unitary gas, the total number density $N = N_a$; for its mixtures in a buffer gas of density N, N_a is much less than N.

The density-reduced electron attachment coefficient of C_2F_6 has been measured by a number of investigators.[47,64-66] Figure 18 shows these measurements which were made at temperatures ranging from 293 K to 300 K. Hunter *et al.*[65] quoted uncertainties ranging from about ±4% at low E/N to about ±7% at the highest E/N values at which they made measurements. Naidu and Prasad[47] quoted uncertainties of ±10%–±20%, and the Božin and Goodyear[66] measurements have an anticipated uncertainty of probably ±10%. The stated uncertainties of the data of Bortnik and Panov[64] are difficult to determine but appear to be between ±5% and ±10%. Only the data of Hunter *et al.*[65] extend to low E/N. In the region where the data overlap there is considerable variation which seems to be outside of the quoted combined uncertainties. In particular, the data of Božin and Goodyear[66] are lower than the rest around $E/N = 200\times10^{-21}$ V m^2 and the data of Hunter *et al.*[65] are higher than the rest above 300×10^{-21} V m^2. The Hunter *et al.*[65] data seem to indicate an enhancement in this E/N range that none of the other sets of measurements indicate. This behavior was present in their

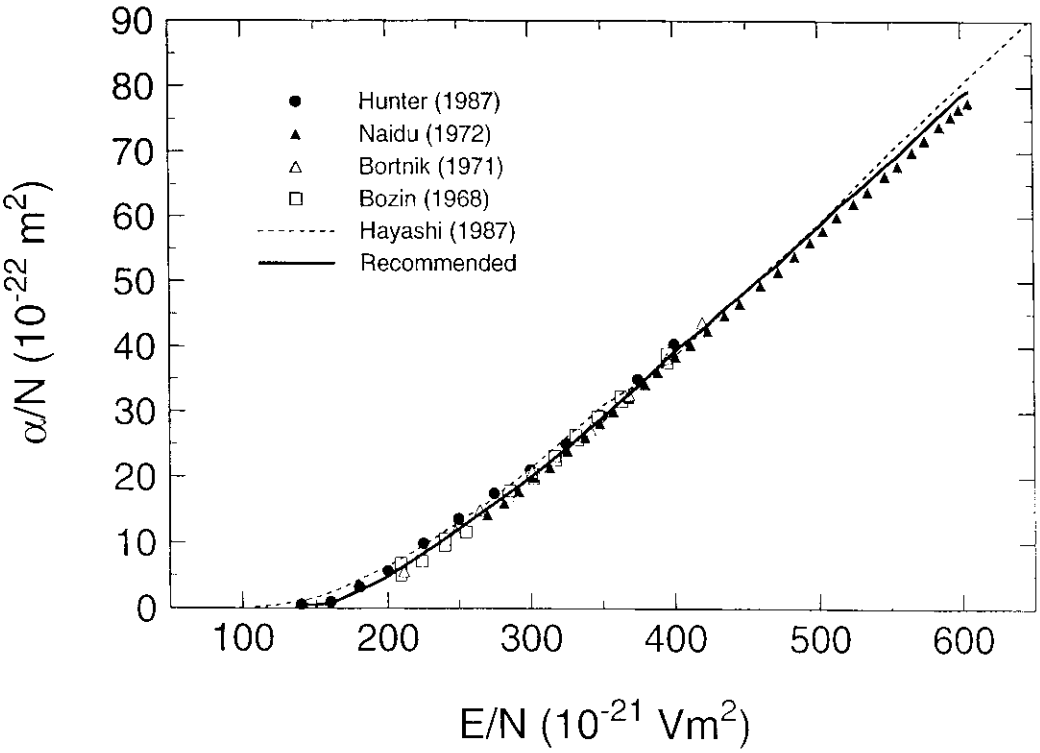

FIG. 14. Density-reduced ionization coefficient (α/N) as a function of E/N for C_2F_6. (●) Ref. 65; (△) Ref. 64; (□) Ref. 66; (▲) Ref. 47; (---) Ref. 42; (—) recommended.

measurements at both room temperature and at 500 K. Hunter *et al.*[65] suggested that the difference between their data using a pulsed Townsend technique and the other measurements using the steady-state Townsend method may be the neglect of secondary electron production processes in the analysis of the current growth curves in the steady-state measurements.

TABLE 12. Recommended density-reduced ionization coefficients, α/N, for C_2F_6

E/N (10^{-21} V m^2)	(α/N) (10^{-22} m^2)
140	0.51
160	0.85
180	2.71
200	4.83
220	7.65
240	10.56
260	13.63
280	16.74
300	19.95
320	23.43
340	27.20
360	31.04
380	35.01
400	39.21
420	42.86
440	46.82
460	50.64
480	54.53
500	58.54
550	68.44
600	78.61

Figure 18 also shows the η/N values calculated by Hayashi and Niwa[42] from their Boltzmann code analysis. The agreement with the experimental values varies significantly with E/N.

To determine a recommended set of η/N data we performed a least-squares fit to all four sets of experimental data in Fig. 18 between 200×10^{-21} V m^2 and 400×10^{-21} V m^2 excluding the two lowest E/N data points of Božin and Goodyear and the highest three E/N data points of Hunter *et al.* since these fall outside of the combined uncertainty. We then extended the recommended curve to lower E/N by normalizing the data of Hunter *et al.* to the average value of η/N at $E/N=200\times10^{-21}$ V m^2 and to higher E/N by normalizing the data of Naidu and Prasad to the average value of η/N at 400×10^{-21} V m^2. The solid line in Fig. 18 represents the curve obtained as has just been described. Recommended values from the solid line are given in Table 15.

There has been only one measurement of $\eta/N(E/N)$ at a temperature above ambient, namely that by Carter *et al.*[67] at 500 K. These measurements are compared with the room temperature data in Fig. 19. The values of η/N at 500 K are higher than at 300 K due to the enhancement of dissociative electron attachment at the elevated temperature (Sec. 6.6.).

Values of $\eta/N_a(E/N)$ in mixtures of C_2F_6 with Ar or CH_4 have been reported by Hunter *et al.*[14] and by Carter *et al.*[67]

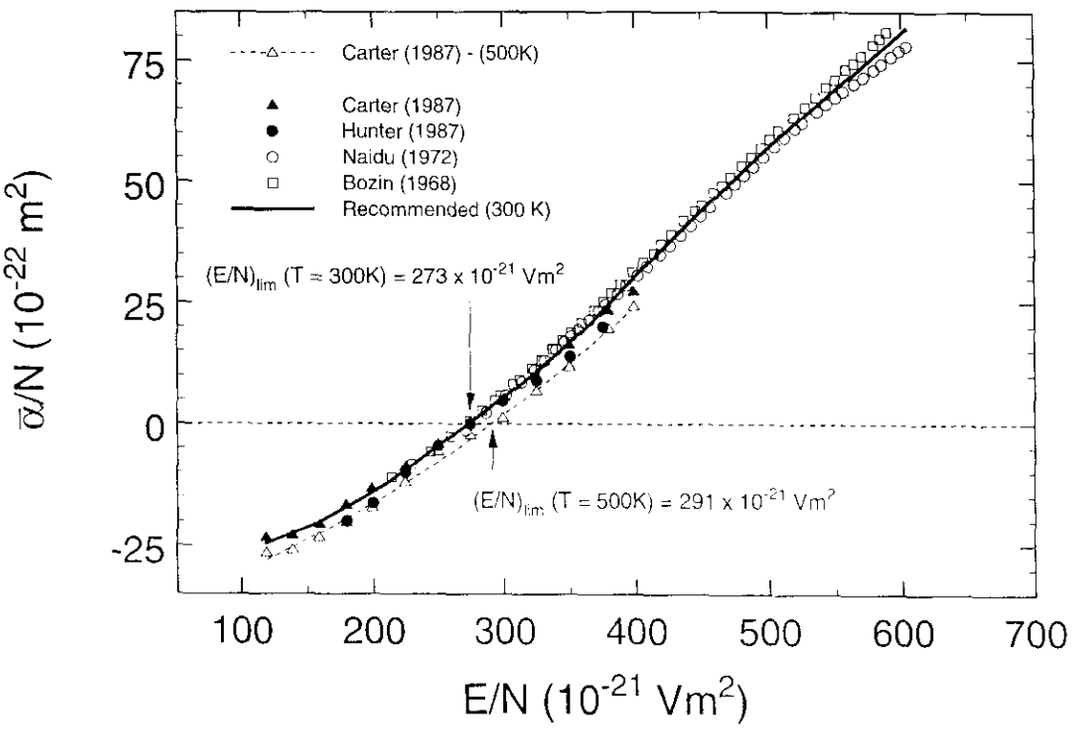

FIG. 15. Density-reduced effective ionization coefficient, $\bar{\alpha}/N=(\alpha-\eta)/N$ as a function of E/N for C_2F_6. Room temperature data: (▲) Ref. 67 (300 K); (●) Ref. 65 (300 K); (○) Ref. 47 (293 K); (□) Ref. 66 (293 K); (—), recommended. Data at 500 K: (△), difference between the values of α/N and η/N reported by Carter *et al.* (Ref. 67) at this temperature. Also indicated in the figure are the limiting values of E/N at 300 K and 500 K.

TABLE 13. Recommended effective ionization coefficients, $(\alpha-\eta)/N$, for C_2F_6

E/N (10^{-21} V m^2)	$(\alpha-\eta)/N$ (10^{-22} m^2)
120	−24.5
125	−24.0
130	−23.5
140	−22.4
160	−20.0
180	−17.1
200	−14.0
220	−10.4
240	−6.34
260	−2.45
280	1.43
300	5.47
320	9.75
340	14.3
360	19.3
380	24.7
400	30.4
420	35.9
440	41.3
460	46.7
480	51.9
500	57.0
525	63.2
550	69.1
575	74.9
600	80.7

6.2. Total electron attachment rate constant, $k_{a,t}$

The density-reduced electron attachment coefficient $\eta/N(E/N)$ is related to the total electron attachment rate constant by

$$k_{a,t}(E/N)=\eta/N(E/N)\times w(E/N), \tag{5}$$

TABLE 14. Values of $(E/N)_{lim}$[a,b] for C_2F_6

$(E/N)_{lim}$ (10^{-21} V m^2)	Reference
274.2 (298K)	70, 71
274.6 (373K)	
275.1 (423K)	
275.9 (473K)	
276.3 (523K)	
277.1 (573K)	
275	12, 65
277	64
277	47
271	66
271[c]	72
278[c]	73
285[c]	74
289[c]	75
322[c]	76

[a]All values are for room temperature unless otherwise noted.
[b]From the least-squares fit to the 300 K data in Fig. 15 we obtained a value for $(E/N)_{lim}$ equal to 273×10^{-21} V m^2 which is recommended.
[c]Uniform field breakdown measurements.

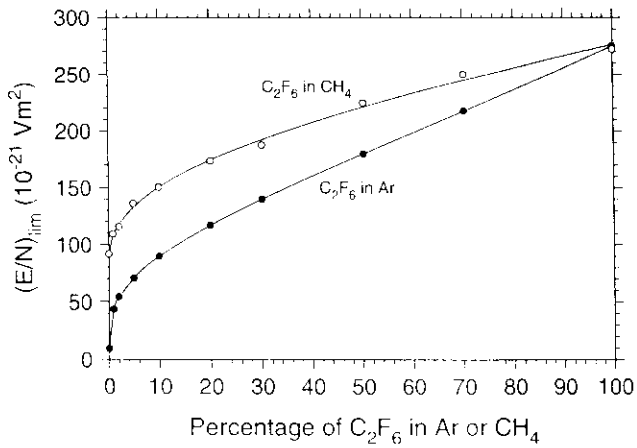

FIG. 16. $(E/N)_{lim}$ as a function of percentage of C_2F_6 in Ar or CH_4 (data of Ref. 12).

where $w(E/N)$ is the electron drift velocity of the unitary gas (or gas mixture when measurements are made of η/N_a, N_a being the number density of the electron attaching gas). There has been only the one measurement of $k_{a,t}$ in pure C_2F_6 by Hunter *et al.*[65] at 300 K. This measurement is shown in Fig. 20. Similar measurements have been made for mixtures of C_2F_6 with argon by Hunter and Christophorou[83] and Spyrou and Christophorou.[84] The measurements in mixtures are shown as a function of E/N in Fig. 21(a), and as a function of the mean electron energy in Fig. 21(b). The plot in Fig. 21(b) was possible because the measurements in the argon mixtures were made at very small concentrations of C_2F_6. This allowed determination of the mean electron energy as a function of E/N from the known electron energy distribution functions as a function of E/N in argon. Each of the two sets of data probably has a total uncertainty of $\pm 10\%$. Their average is shown by the solid line in Fig. 21(b) and is listed in Table 16 as our recommended set of values for the total electron attachment rare constant for C_2F_6 as a function of the mean electron energy.

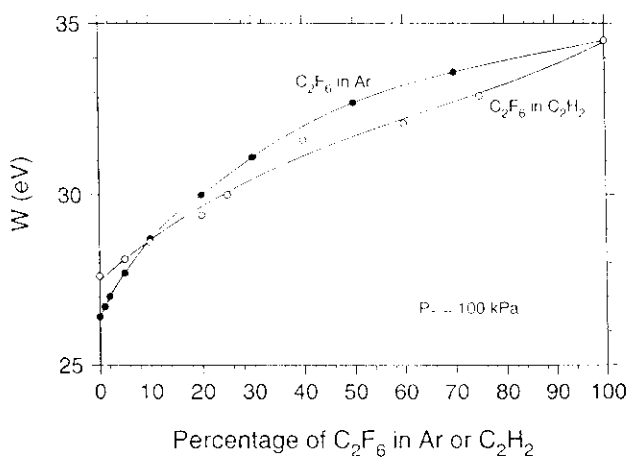

FIG. 17. Energy, W, needed to produce an electron-ion pair by α particles (initial energy 5.1 MeV) in mixtures of C_2F_6 with Ar or C_2H_2. The total pressure of the mixtures was 100 kPa [data of Reinking *et al.* (Ref. 78)].

6.3. Thermal value of the total electron attachment rate constant, $(k_{a,t})_{th}$

The value of $k_{a,t}(E/N)$ when the electron energy distribution function $f(\varepsilon,E/N)$ is Maxwellian, $f_M(\varepsilon,T)$, i.e., when $E/N \rightarrow 0$, and $f(\varepsilon,E/N)$ is characteristic of only the gas temperature T, is referred to as the total thermal electron attachment rate constant $(k_{a,t})_{th}$ and is given by

$$(k_{a,t})_{th} = (2/m)^{1/2} w^{-1} \int_0^\infty f_M(\varepsilon,T)^{1/2} \sigma_{a,t}(\varepsilon) d\varepsilon. \quad (6)$$

Table 17 lists reported[65,83,85,86] values of $(k_{a,t})_{th}$ measured at $T \approx 300$ K. These values are very small ($< 1.6 \times 10^{-13}$ cm^3 s^{-1}) and may well be due to or affected by traces of strongly electronegative impurities.

6.4. Total electron attachment cross section, $\sigma_{a,t}(\varepsilon)$

The main source of recent total electron attachment cross sections for C_2F_6 is the room temperature swarm-unfolded data of Christophorou and co-workers.[83,84] These data are presented in Fig. 22. Figure 22 also shows the relative total electron attachment cross section as determined in an electron beam experiment by Spyrou and Christophorou[84] normalized to the peak of their swarm-unfolded total electron attachment cross section. Its shape agrees reasonably well with the swarm-unfolded data. The two major dissociative attachment fragment negative ions of C_2F_6 (see Sec. 6.5.) are F^- and CF_3^-.

Also available in the literature are the results of three early, low resolution, electron beam experiments. An early beam study by Bibby and Carter[56] reported a cross section value of 1.76×10^{-20} m^2 for F^- and 0.43×10^{-20} m^2 for CF_3^- at 3.75 eV. The sum of these two peak cross section values for the two fragments is 2.19×10^{-20} m^2 which is more than ten times larger than the more recent data in Fig. 22 indicate. The results of a second beam experiment by Kurepa[57] are also more than ten times the swarm-determined total electron attachment cross sections. Neither of these measurements are considered to be reliable in light of the more recent measurements, and therefore are not presented in Fig. 22. The third beam study is that of Harland and Franklin[87] who found the maximum intensity for the two main fragment anions F^- and CF_3^- to be at 4.3 eV and 4.4 eV, respectively. At these energy values they reported the respective cross sections to be 5×10^{-22} m^2 and 1×10^{-22} m^2. Since these two ions are by far the two most intense fragment negative ions, we compare the sum (6×10^{-22} m^2) of the two with the peak values of the total electron attachment cross section (at 4.35 eV) in Fig. 22. It is about a factor of 2 lower than the other data.

The average of the two sets of swarm-unfolded measurements by Christophorou and co-workers is shown in Fig. 22 by the solid line. Data taken off this curve are listed in Table 18 as our recommended values for the $\sigma_{a,t}(\varepsilon)$ of C_2F_6.

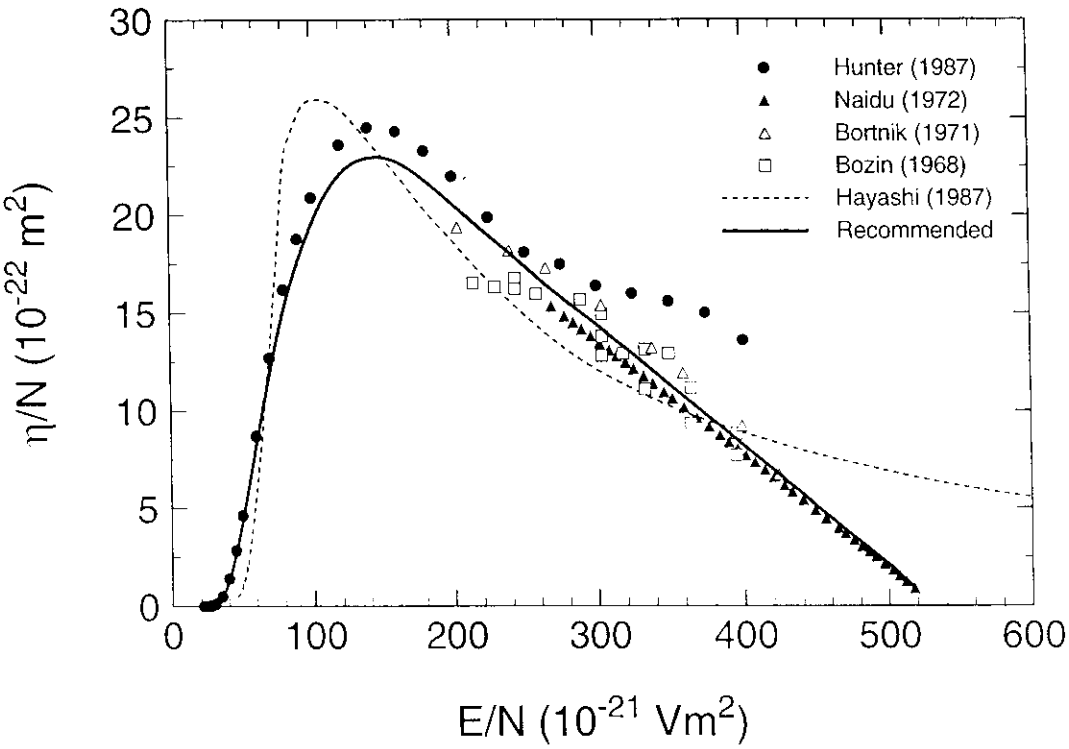

FIG. 18. Density-reduced electron attachment coefficient, η/N as a function of $E/N(T=293-300\ \mathrm{K})$ for C_2F_6. Measurements: (●) Ref. 65; (▲) Ref. 47; (△) Ref. 64; (□) Ref. 66. Calculations: (---), Ref. 42. Recommended: (—).

6.5. Dissociative electron attachment fragment anions

Electron beam studies of negative ion formation by electron impact on C_2F_6 have shown that below 10 eV three fragment anions (F^-, CF_3^- and $C_2F_5^-$) are produced via a prominent broad negative ion resonance in the energy range 2–7 eV. The decomposition channels were described[87,88] as

$$C_2F_6{}^* \rightarrow F^- + C_2F_5 \quad (7)$$

$$\rightarrow CF_3^- + CF_3 \quad (8)$$

$$\rightarrow C_2F_5^- + F. \quad (9)$$

The relative yield of the F^-, CF_3^-, and $C_2F_5^-$ fragment anions as measured by Spyrou *et al.*[88] is shown in Fig. 23(a). A comparison of the relative intensities of these three ions and their energetics, as have been measured by various groups, is given in Table 19. Clearly, F^- is the most abundant species and $C_2F_5^-$ the least abundant. The relative cross section curves for F^- and CF_3^- are broad, nearly identical in shape, and peak at about the same energy (4.3 eV), indicating that the two ions are generated by the same negative ion state. In contrast, the relative cross section for $C_2F_5^-$ is much narrower and peaks at a higher energy (4.8 eV) indicating that it may originate from a different negative ion state than the other two fragment anions. An energy analysis of the F^- anion by Harland and Franklin[87] revealed that the translational energy curve for F^- has a break between 4 eV and 5 eV. They interpreted this as resulting from the formation of F^- ions from a different negative ion state. More recently, Weik and Illenberger[39] revisited this point and suggested that this behavior along with the observation that the $C_2F_5^-$ ions form only at energies above 4 eV indicates the existence of two energetically overlapping negative ion states in this energy range, the higher energy one being "more C–F antibonding." According to Weik and Illenberger, calculations by Weik[40] predict $3a_{2u}(\sigma^*_{CC})$ and $3a_{2u}(\sigma^*_{CF})$ virtual molecular orbitals in this energy range (see Table 3 for the assignments of Tagaki *et al.*[38] and Ishii *et al.*[35]). The data of Weik and Illenberger[39] for production of F^- and $C_2F_5^-$ are presented in Fig. 23(b). They are consistent with those in Fig. 23(a) as to the production of F^- and $C_2F_5^-$ in the energy region between 2 eV and 7 eV, but they extend to higher energies. The yield of F^- in Fig. 23(b) indicates maxima at 9.3 eV and 12.5 eV. The maximum at 9.3 eV is consistent with electron scattering measurements (see Table 3).

No $C_2F_6^-$ parent negative ion has been observed under single collision conditions. However, a recent report[37] indicated the observation of the $C_2F_6^-$ ion in studies of electron attachment to pure C_2F_6 clusters. It is unlikely that this is an indication that the electron affinity of C_2F_6 is positive. Most probably the lowest negative ion state of C_2F_6 is the one with vertical energy at 4.0 eV (see Table 3). The $C_2F_6^-$ observed in the Lehmann *et al.*[37] study is likely to be an excited $C_2F_6^-{}^*$ species formed in the lowest negative ion state that has a potential minimum and sufficiently long lifetime to be detected in the mass spectrometer. It may thus be inferred

TABLE 15. Recommended values of the density-reduced electron attachment coefficient, η/N, for C_2F_6

E/N (10^{-21} V m^2)	$(\eta)/N$ (10^{-22} m^2)
22	0.001
25	0.008
30	0.09
35	0.46
40	1.31
45	2.64
50	4.32
60	8.14
70	11.9
80	15.2
90	17.6
100	19.6
120	22.1
140	22.9
160	22.7
180	21.8
200	20.6
220	19.3
240	18.0
260	16.7
280	15.5
300	14.4
320	13.2
340	11.9
360	10.7
380	9.45
400	8.20
420	6.94
440	5.71
460	4.47
480	3.25
500	2.09
515	1.09

from these observations that the C_2F_6* from clusters lives longer than 1 μs, while the C_2F_6* formed under isolated conditions lives for just a few fs.[88]

Finally, it is noted that besides the fragment anions F^-, CF_3^-, and $C_2F_5^-$, MacNeil and Thynne[89] reported observation of CF^-, F_2^-, C_2F^-, and CF_2^-.

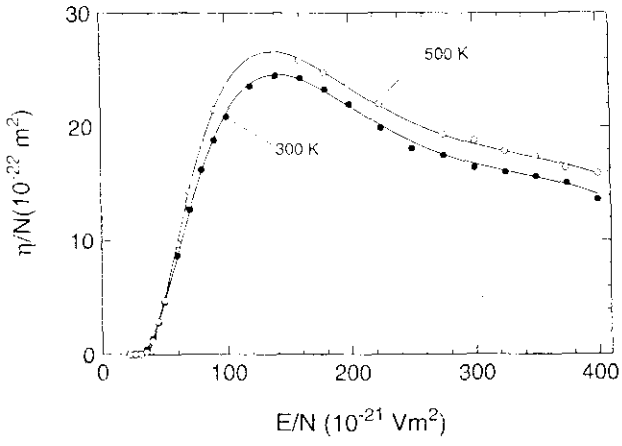

FIG. 19. Density-reduced electron attachment coefficient, η/N, as a function of E/N at $T = 300$K [(●) Ref. 65] and $T = 500$K [(○) Ref. 67] for C_2F_6.

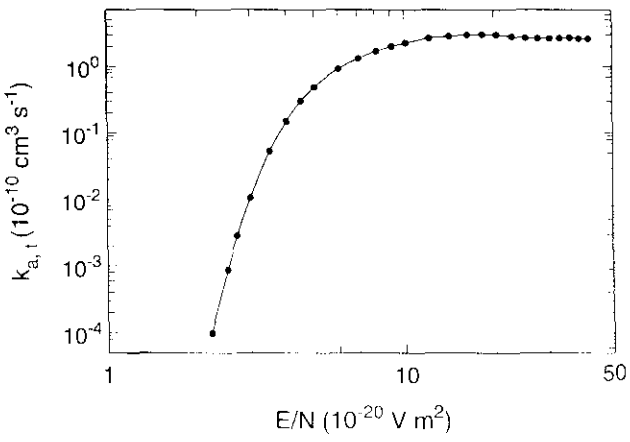

FIG. 20. Total electron attachment rate constant as a function of E/N, $k_{a,t}(E/N)$, for pure C_2F_6 (data of Ref. 65).

6.6. Effect of temperature on $k_{a,t}(\langle\varepsilon\rangle)$ and $\sigma_{a,t}(\varepsilon)$

The only study on the effect of temperature on electron attachment to C_2F_6 appears to be by Spyrou and Christophorou.[84] These investigators measured the $k_{a,t}(E/N)$ of C_2F_6 in mixtures of C_2F_6 with argon for temperatures ranging from 300 K to 750 K. Their results are shown in Fig. 24. The increase of the total electron attachment rate constant with increasing temperature is only modest because the dissociating negative ion state lies well above thermal energies

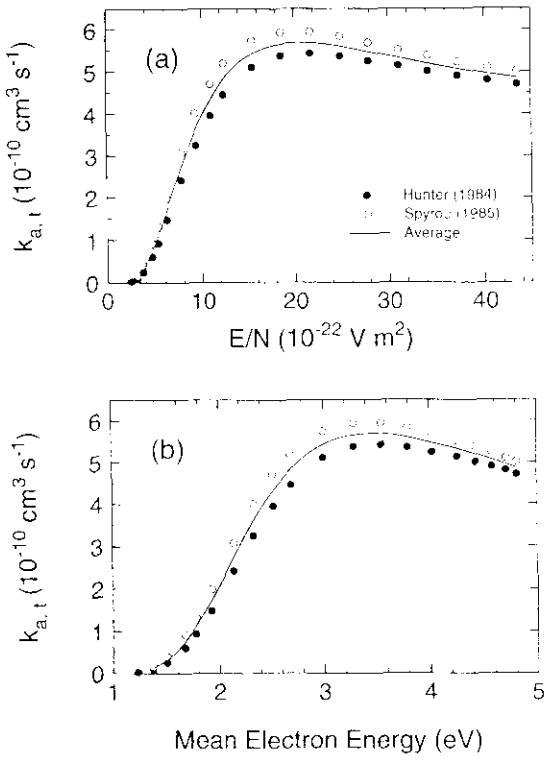

FIG. 21. Total electron attachment rate constant, $k_{a,t}$, for C_2F_6 measured in mixtures of C_2F_6 in argon buffer gas (a) as a function of E/N and (b) as a function of the mean electron energy $\langle\varepsilon\rangle$. (●) Ref. 83; (○) Ref. 84; (—), average.

TABLE 16. Recommended total electron attachment rate constant $k_{a,t}(\langle\varepsilon\rangle)$, as a function of the mean electron energy $\langle\varepsilon\rangle$ for C_2F_6 measured in mixtures of C_2F_6 with argon[a]

Mean electron energy (eV)	$k_{a,t}(\langle\varepsilon\rangle)$ $(10^{-10}\ cm^3\ s^{-1})$
1.37	0.14
1.50	0.33
1.67	0.77
1.77	1.13
1.92	1.74
2.14	2.75
2.33	3.63
2.52	4.34
2.69	4.83
3.00	5.43
3.29	5.66
3.55	5.69
3.80	5.61
4.03	5.47
4.26	5.33
4.43	5.20
4.58	5.07
4.71	4.95
4.81	4.86

[a]From Fig. 21(b).

TABLE 17. Thermal ($T \approx 300$ K) values of the total electron attachment rate constant, $(k_{a,t})_{th}$, for C_2F_6

$(k_{a,t})_{th}$ $(cm^3\ s^{-1})$	Reference
$<1\times10^{-16}$	65, 85
$<1\times10^{-13}$	83
$<1.6\times10^{-13}$	86

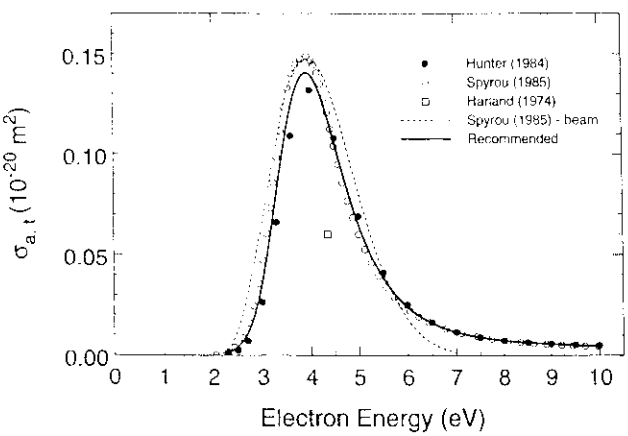

FIG. 22. Total electron attachment cross section as a function of electron energy, $\sigma_{a,t}(\varepsilon)$, for C_2F_6. Swarm-unfolded data: (●) Ref. 83; (○) Ref. 84. Beam relative data normalized to the swarm-unfolded data at the maximum: (----), Ref. 84. (□) Ref. 87, (---), recommended cross section.

TABLE 18. Recommended total electron attachment cross section, $\sigma_{a,t}(\varepsilon)$, for C_2F_6 ($T = 300$ K)

Electron energy (eV)	$\sigma_{a,t}(\varepsilon)$ $(10^{-20}\ m^2)$
2.0	0.0001
2.25	0.0007
2.5	0.0044
2.75	0.013
3.0	0.036
3.25	0.073
3.5	0.11
4.0	0.14
4.5	0.11
5.0	0.064
5.5	0.039
6.0	0.024
6.5	0.016
7.0	0.012
7.5	0.0091
8.0	0.0074
8.5	0.0064
9.0	0.0057
9.5	0.0051
10.0	0.0046

(Tables 3 and 19). Spyrou and Christophorou[84] determined total dissociative attachment cross sections for C_2F_6 as a function of temperature by unfolding the rate constants in Fig. 24 and using the known electron energy distribution

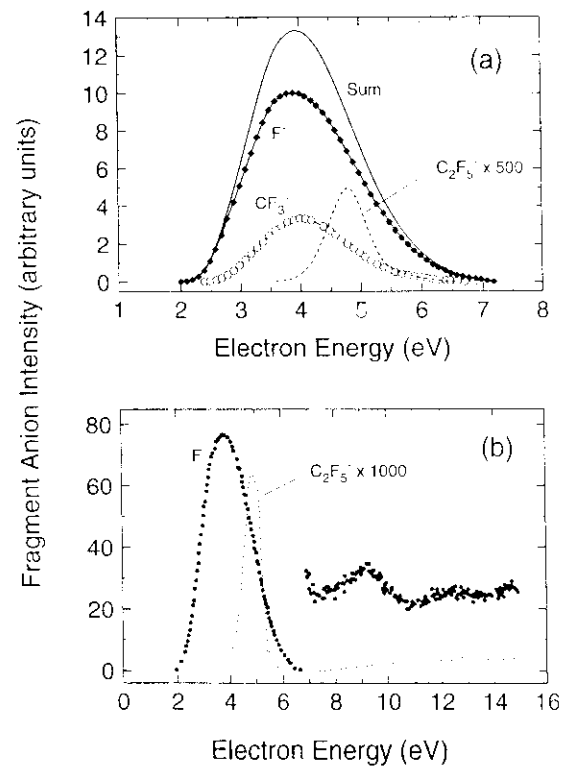

FIG. 23. (a) Relative yield of the fragment ions F^-, CF_3^-, and $C_2F_5^-$ as a function of electron energy produced by dissociative electron attachment to C_2F_6 (data of Ref. 88); (b) Relative yield of the fragment ions F^- and $C_2F_5^-$ as a function of electron energy produced by dissociative electron attachment to C_2F_6 (data of Ref. 39).

TABLE 19. Fragment negative ions produced by electron impact on C_2F_6, their energetics, and relative intensities

Fragment anion	Possible reaction	Energy threshold (eV)	Energy of maximum intensity (eV)	Relative abundance	Reference
F^-	$C_2F_6+e\rightarrow F^-+C_2F_5$[a] $C_2F_6+e\rightarrow F^-+C_2F_5^*$ $C_2F_6+e\rightarrow F^-+CF_2+CF_3$ $C_2F_6+e\rightarrow F^-+F+C_2F_4$	2.1±0.2 4.9±0.2	4.3±0.1	100	87
F^-	$C_2F_6+e\rightarrow F^-+C_2F_5$[b]	2.0±0.1	3.9±0.05	100	88
F		2.2	3.75	100	56
CF_3^-	$C_2F_6+e\rightarrow CF_3^-+CF_3$[b,c]	2.2±0.2	4.4±0.1	21	87
CF_3^-		2.4±0.1	4.0±0.05	32	88
CF_3^-		2.8	3.75	24	56
$C_2F_5^-$				1	87
$C_2F_5^-$		3.5±0.1	4.8±0.1	~0.1	88
F		2.25±0.2	3.80±0.2	100	89[d]
CF_3^-		2.7±0.2	3.9±0.2	1.2	
$C_2F_5^-$		4.0±0.2	4.8±0.2	0.01	

[a]Harland and Franklin (Ref. 87) determined a value of (5.5±0.2) eV for the dissociation energy $D(F-C_2F_5)$, (4.6±0.6) eV for the dissociation energy $D(CF_3-CF_3)$, (2.4±0.5) eV for the electron affinity of CF_4, and ~2.9 eV for the excitation energy of C_2F_5. The value obtained by Harland and Franklin for the dissociation energy $D(CF_3-CF_3)$ is in reasonable agreement with the value of (4.18±0.04) eV given earlier by Coomber and Whittle (Ref. 90). The Harland and Franklin values for the dissociation energies $D(F-C_2F_5)$ and $D(CF_3-CF_3)$ are also consistent with those determined from similar studies by Spyrou *et al.* (Ref. 88) (see footnote c of this table). The values for the electron affinity of CF_3 range from 1.36 eV to 3.25 eV and those for C_2F_5 from 2.1 eV to 3.3 eV (see Ref. 91).

[b]Both the peak energies and the values of the energy thresholds shift toward lower energies with increasing temperature (see Sec. 6.6.) The data given are for 300 K. The other entries given in the table are probably also for about 300 K, although in some of the electron beam studies the gas might have been at a higher temperature than ambient via heating from the hot filament in the electron source.

[c]Spyrou *et al.* (Ref. 88) estimated $D(F-C_2F_5)$ to be ≤(5.4±0.15) eV from data on the reaction $C_2F_6+e\rightarrow F^-+C_2F_5$ and ≤(5.6±0.1) eV from data on the reaction $C_2F_6+e\rightarrow F+C_2F_5^-$. From similar data on the reaction $C_2F_6+e\rightarrow CF_3^-+CF_3$, they reported $D(CF_3-CF_3)=(3.8\pm0.1)$ eV.

[d]These authors also reported observation of CF^-, F_2^-, and CF_2^-.

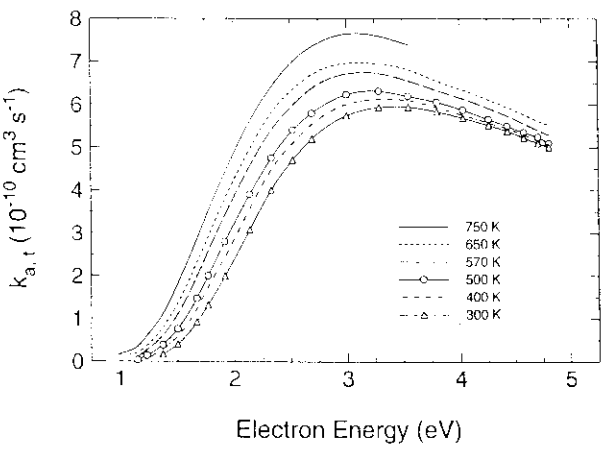

FIG. 24. Total electron attachment rate constant $k_{a,t}(\langle\varepsilon\rangle)$ for C_2F_6 as a function of the gas temperature measured in mixtures with argon (data from Ref. 84).

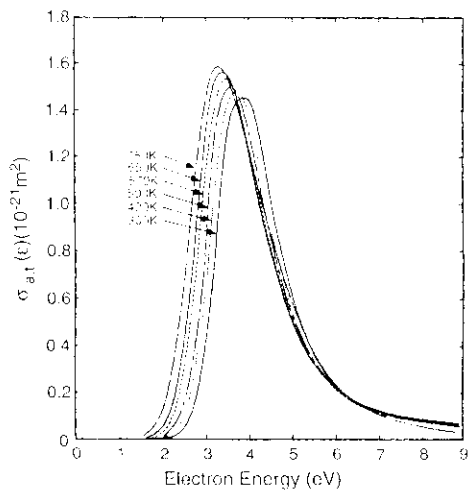

FIG. 25. Total electron attachment cross sections $\sigma_{a,t}(\varepsilon)$ at various temperatures between 300 K and 750 K based on the measurements in Fig. 24 (see the text and Ref. 84).

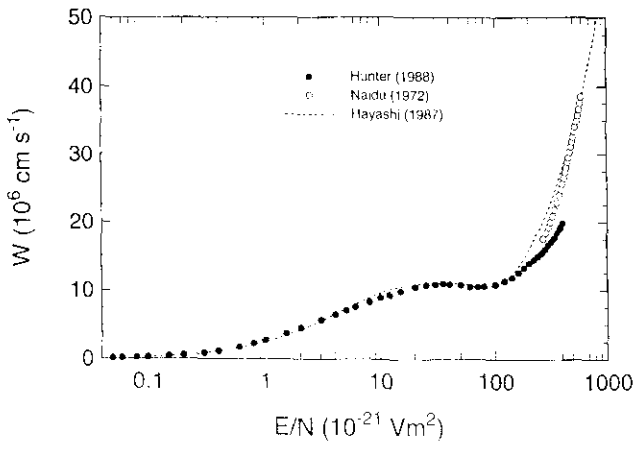

FIG. 26. Electron drift velocity w as a function of E/N for pure C_2F_6. Measurements: (●) ($T = 300$ K) Ref. 92; (○) ($T = 293$ K) Ref. 47. Calculation (---), Ref. 42.

functions in argon. Their findings are reproduced in Fig. 25. The magnitude of $\sigma_{a,1}(\varepsilon)$ increases and its energy threshold decreases with increasing temperature. The single peak in $\sigma_{a,1}(\varepsilon)$ (due to F^- and CF_3^-) shifts from 3.9 eV at 300 K to ~3.3 eV at 750 K and the corresponding onset from 2.3 eV to 1.5 eV.

7. Electron Transport

7.1. Electron drift velocity, w

There have been three measurements of the electron drift velocity, w, of C_2F_6. Two of these[47,92] were performed at room temperature and the other[67] at 500 K. Figure 26 summarizes the room temperature data. The measurements of Hunter *et al.*[92] cover a wide range of E/N values, while the measurements of Naidu and Prasad[47] are restricted to high E/N values (the data plotted in Fig. 26 were taken from the smooth line of their paper). The measurements of Hunter *et al.*[92] have stated maximum uncertainties of ±5% above $(E/N)_{\text{lim}}$, decreasing to ±2% at values of E/N below the onset of electron attachment. Hunter *et al.* corrected their data for the effects of electron attachment, ionization, and diffusion. Naidu and Prasad[47] estimated their uncertainty to be ±5%. Considering the quoted uncertainties, there is disagreement between the two sets of data in the region of overlap. Hunter *et al.*[92] attributed the differences between their data and the data of Naidu and Prasad at high E/N to the uncertainty in the Naidu and Prasad measurements. The latter measurements become uncertain at high E/N because w is large and the electron transit time very short making it difficult to accurately obtain the transit time from oscilloscope tracings, especially when the width of the pulsed light source used to generate the photoelectron pulse is an appreciable fraction of the electron transit time. Another possible source of uncertainty pointed out by Hunter *et al.*[92] is the high background ion current in the Naidu and Prasad experiment. Using the cross section set shown in Fig. 3, Hayashi and Niwa[42] calculated the $w(E/N)$ curve represented by the broken line in Fig. 26, showing agreement with Hunter *et al.* at low E/N and Naidu and Prasad at high E/N. The data of Hunter *et al.* are listed in Table 20 as our recommended set of w values for C_2F_6 in view of the effort made in this study to consider the various sources of errors and to correct for their influence on the measurements.

TABLE 20. Recommended electron drift velocity, $w(T = 300$ K), for C_2F_6[a]

E/N (10^{-17} V cm^2)	w(10^6 cm s^{-1})
0.05	0.147
0.06	0.176
0.08	0.237
0.10	0.295
0.15	0.435
0.20	0.58
0.30	0.87
0.40	1.15
0.60	1.69
0.80	2.23
1.0	2.71
1.5	3.69
2.0	4.54
3.0	5.68
4.0	6.51
5.0	7.13
6.0	7.62
8.0	8.36
10.0	8.92
12.0	9.3
15.0	9.9
20.0	10.5
25.0	10.8
30.0	10.9
35.0	11.0
40.0	10.9
50.0	10.8
60.0	10.5
70.0	10.5
80.0	10.6
100.0	10.9
120.0	11.4
140.0	11.9
160.0	12.6
180.0	13.3
200.0	14.0
220.0	14.5
240.0	15.0
260.0	15.4
280.0	16.0
300.0	16.6
320.0	17.1
340.0	17.6
360.0	18.4
380.0	19.1
400.0	19.8

[a]Data of Ref. 92.

The electron drift velocity measurements at 300 K and 500 K reported by Carter *et al.*[67] are shown in Fig. 27. The electron drift velocity is lower at the higher temperature. This is also evident in Table 21 showing the thermal values of the density-normalized electron mobility $(\mu N)_{\text{th}}$ for C_2F_6 measured as a function of temperature.[52] A rather profound decrease is observed that may be due to the effect on electron

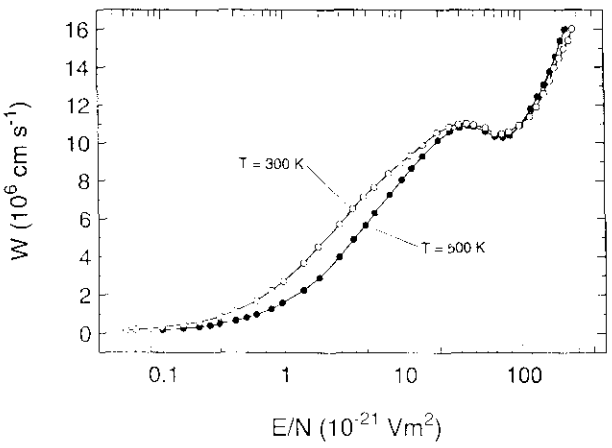

FIG. 27. Electron drift velocity w as a function of E/N for pure C_2F_6 at 300 K (○) and 500 K (●) (data of Ref. 67).

TABLE 21. Measured density-normalized thermal-electron mobilities, $(\mu N)_{th}$, for C_2F_6 as a function of gas temperature[a]

Temperature (K)	$(\mu N)_{th}$ (10^{23} V^{-1} cm^{-1} s^{-1})
300	2.92
400	2.20
500	1.63
600	1.23
700	0.94

[a]From Ref. 52.

motion[52] of enhanced electron scattering from vibrationally excited $C_2F_6^*$ molecules.

Measurements have also been made of the w in mixtures of C_2F_6 with various gases such as Ar and CH_4. These measurements were partially motivated by the development of fast mixtures (mixtures with very large electron drift velocities) for use in gas pulse-power switches (see Sec. 1). A sample of these data taken from Carter *et al.*[67] are shown in Fig. 28. It is interesting to note the negative differential conductivity (decrease in w with increasing E/N) exhibited by these mixtures for certain E/N regions that depend on mixture composition.

7.2. Ratio of the transverse electron diffusion coefficient to electron mobility, D_T/μ

There have been two sets of measurements of $D_T/\mu(E/N)$ for pure C_2F_6, one by Naidu and Prasad[47] and the other by Hunter *et al.*[14] The Naidu and Prasad data were taken at a temperature of 293 K, pressures ≤ 0.4 kPa, and E/N values in the range 270×10^{-21} V m^2 to about 608×10^{-21} V m^2. The quoted uncertainty in their data ranges from $\pm 5\,\%$ at the lowest values of E/N to $\pm 3\,\%$ at the highest E/N values at which they made measurements. Points taken off the solid curve for C_2F_6 in Fig. 2 of their paper are plotted in Fig. 29. Hunter *et al.*[14] measured D_T/μ for pure C_2F_6 in a lower E/N range (0.6×10^{-21}–389×10^{-21} V m^2). No estimate of the uncertainty of their data or the temperature at which the measurements were made was given. However, since the mea-

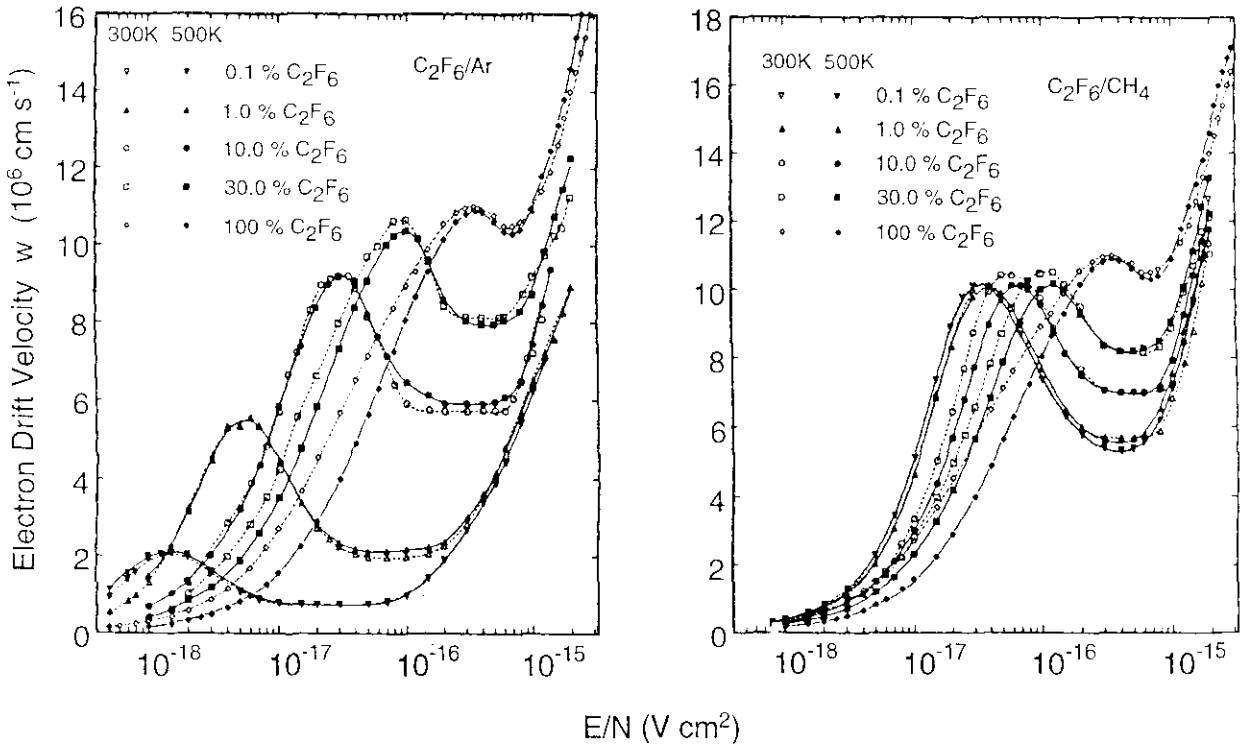

FIG. 28. Electron drift velocity w as a function of E/N for mixtures of C_2F_6 with Ar [Fig. 28(a)] and with CH_4 [Fig. 28(b)] at two gas temperatures (300 K and 500 K) (data of Ref. 67).

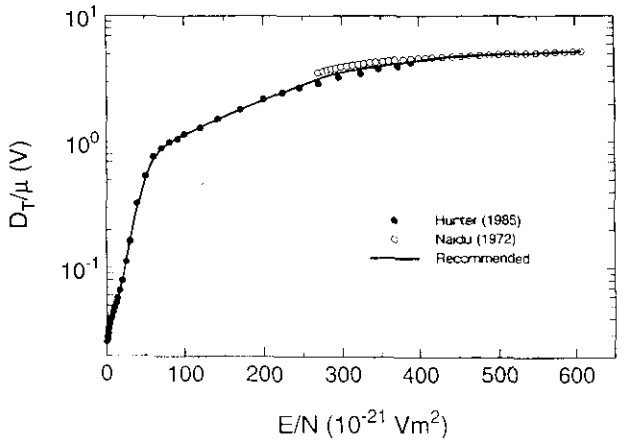

FIG. 29. Transverse electron diffusion coefficient to electron mobility ratio, D_T/μ, measured at 293 K for C_2F_6: (●) Ref. 14; (○) Ref. 47; (—) recommended.

surements were made using the D_T/μ apparatus at the Australian National University,[93] the uncertainty is expected to be only a few per cent and the temperature ~293 K. Their measurements are also plotted in Fig. 29. In the E/N range, where the data of Hunter *et al.* overlap the values of Naidu and Prasad, the latter lie higher. We fitted the two sets of measurements as shown by the solid line in Fig. 29. Data taken off the solid line are listed in Table 22 as our recommended set of D_T/μ for C_2F_6.

Measurements have also been reported[12] of the $D_T/\mu(E/N)$ for the mixture 10% C_2F_6/90% CH_4. These are shown in Fig. 30, where they are compared with the results of a Boltzmann code analysis for this mixture by Hayashi and Niwa.[42] The overall agreement is reasonable although the calculated values do not converge to the low E/N asymptotic limit of kT/e.

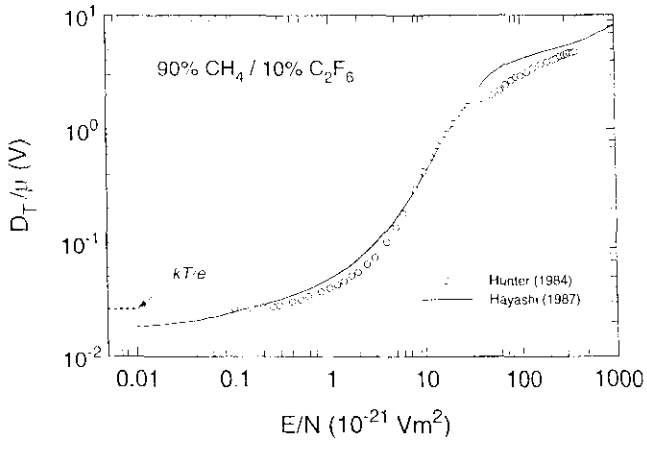

FIG. 30. Transverse electron diffusion coefficient to electron mobility ratio, D_T/μ, for the mixture 10% C_2F_6/90% CH_4. Measurements (T = 293 K): (○) Ref. 12; Calculation: (—), Ref. 42.

8. Summary of Cross Sections and Coefficients

The cross sections that have been designated as recommended or suggested in this paper are plotted in Fig. 31. These include the recommended cross sections of:

(i) integral elastic electron scattering cross section, $\sigma_{e,int}(\varepsilon)$ in Table 7 (Fig. 7);
(ii) total dissociation cross section, $\sigma_{diss,t}(\varepsilon)$ in Table 11 (Fig. 13);
(iii) total electron attachment cross section, $\sigma_{a,t}(\varepsilon)$ in Table 18 (Fig. 22),

and the suggested cross sections of:

(iv) momentum transfer cross section, $\sigma_m(\varepsilon)$ in Table 5 (Fig. 5);
(v) total ionization cross section, $\sigma_{i,t}(\varepsilon)$ in Table 10 (Fig. 12); and
(vi) total scattering cross section $\sigma_{sc,t}(\varepsilon)$ in Table 4 (Fig. 4).

These data are reasonably consistent within the stated uncertainties, with the only apparent discrepancy being that the $\sigma_{e,int}(\varepsilon)$ exceeds the $\sigma_{sc,t}(\varepsilon)$ data near 15 eV. The differential elastic electron scattering cross section data, $\sigma_{e,diff}(\varepsilon)$ in Table 6 (Fig. 6) are not shown in Fig. 31 but are also recommended.

The following coefficients are recommended:

(i) density-reduced ionization coefficient, α/N in Table 12 (Fig. 14);
(ii) effective ionization coefficient, $(\alpha-\eta)/N$ in Table 13 (Fig. 15);
(iii) density-reduced electron attachment coefficient, η/N in Table 15 (Fig. 18);
(iv) total electron attachment rate constant, $k_{a,t}$ in Table 16 (Fig. 21);
(v) electron drift velocity, w in Table 20 (Fig. 26); and
(vi) ratio of transverse electron diffusion coefficient to electron mobility, D_T/μ in Table 22 (Fig. 29).

All of these data are available via the WorldWide Web at http://www.eeel.nist.gov/811/refdata.

9. Needed Data

There are no published experimental data for the cross section, $\sigma_{diss,neut}(\varepsilon)$, for dissociation of the C_2F_6 molecule into neutral fragments by electron impact, or for other inelastic processes such as vibrational and electronic excitation. Additionally, there is a need to validate the recommended and suggested cross sections that are based on single experimental measurements such as $\sigma_m(\varepsilon)$, $\sigma_{e,int}(\varepsilon)$, $\sigma_{diss,t}(\varepsilon)$, and $\sigma_{sc,t}(\varepsilon)$. These data also need to be extended over a greater energy range, particularly toward lower energies. Improved uncertainties are also desirable for all of the presented data, especially for the total ionization cross section $\sigma_{i,t}(\varepsilon)$.

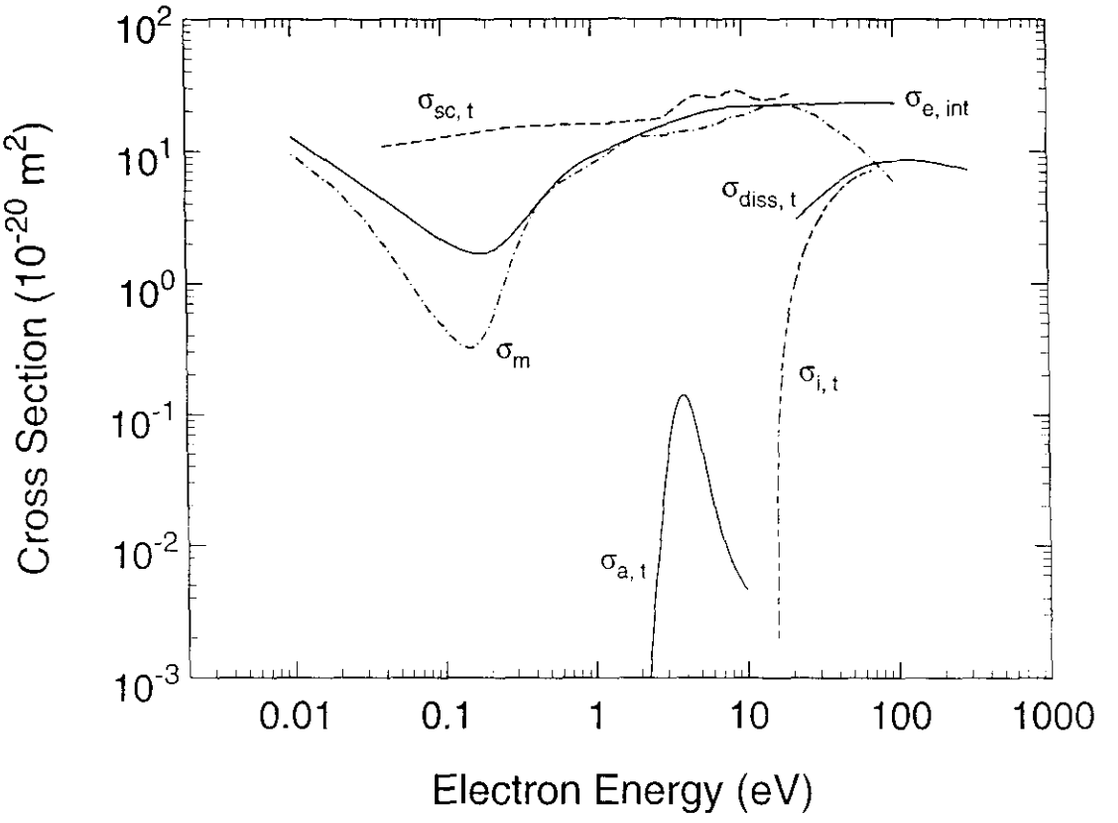

FIG. 31. Recommended and suggested cross section values for C_2F_6.

TABLE 22. Recommended transverse electron diffusion coefficient to electron mobility ratio, D_T/μ, as a function of E/N for C_2F_6

E/N (10^{-21} V m^2)	D_T/μ (V)
1.0	0.029
2.0	0.033
3.0	0.035
4.0	0.038
5.0	0.040
6.0	0.041
7.0	0.043
8.0	0.045
9.0	0.047
10.0	0.049
15	0.060
20	0.080
30	0.161
40	0.305
50	0.511
60	0.712
70	0.868
80	0.967
90	1.05
100	1.13
150	1.59
200	2.15
250	2.83
300	3.56
350	4.00
400	4.43
450	4.77
500	4.93
550	5.07
600	5.20

The need for more coefficient data is minimal. Improved uncertainties for the values of η/N are desirable at all E/N, while improved uncertainties at high E/N would be beneficial for the other coefficients and transport parameters.

10. Acknowledgments

The authors thank J. Verbrugge for valuable assistance with the literature, and Dr. J Moore, J. Sanabia, S. Motlagh, Dr. R. Merz, Dr. F. Linder, and Dr. Y.-K. Kim for providing their data prior to publication.

11. References

[1] L. G. Christophorou, J. K. Olthoff, and M. V. V. S. Rao, J. Phys. Chem Ref. Data **25**, 1341 (1996).
[2] L. G. Christophorou, J. K. Olthoff, and M. V. V. S. Rao, J. Phys. Chem Ref. Data **26**, 1 (1997).
[3] L. G. Christophorou, J K. Olthoff, and Y. Wang, J. Phys. Chem. Ref Data **26**, 1205 (1997).
[4] H.-H. Park, K.-H. Kwon, J.-L. Lee, K.-S. Suh, O.-J. Kwon, K.-I. Cho, and S.-C. Park, J. Appl. Phys. **76**, 4596 (1994).
[5] D. L. Flamm, in *Gaseous Dielectrics V*, edited by L. G. Christophorou and D. W. Bouldin (Pergamon, New York, 1987), p. 317.
[6] J. W. Coburn and E. Kay, J. Vac. Sci. Technol. **16**, 407 (1979).
[7] M. J. Kushner, J. Appl. Phys. **53**, 2923 (1982).
[8] M. O. de Beeck, M. Goethals, and L. Van den hove, J. Electrochem. Soc **139**, 2644 (1992).

[9] M. Haverlag, A. Kono, G. M. W. Kroesen, and F. J. de Hoog, Mater. Sci. Forum **140–142**, 235 (1993).
[10] L. G. Christophorou, S. R. Hunter, J. G. Carter, and R. A. Mathis, Appl. Phys. Lett. **41**, 147 (1982).
[11] P. Bletzinger, in XVI International Conference on Phenomena in Ionized Gases, Contributed Papers, Vol. 2, edited by W. Böttcher, H. Wenk, and E. Schulz-Gulde, Düsseldorf, Germany, August 29–September 2, 1983, p. 218.
[12] S. R. Hunter, J. G. Carter, L. G. Christophorou, and V. K. Lakdawala, in *Gaseous Dielectrics IV*, edited by L. G. Christophorou and M. O. Pace (Pergamon, New York, 1984), p. 224.
[13] V. E. Scherrer, R. J. Commisso, R. F. Fernsler, and I. M. Vitkovitsky, in *Gaseous Dielectrics IV*, edited by L. G. Christophorou and M. O. Pace (Pergamon, New York, 1984), p. 238.
[14] S. R. Hunter, J. G. Carter, and L. G. Christophorou, J. Appl. Phys. **58**, 3001 (1985).
[15] R. J. Commisso, R. F. Fernsler, V. E. Scherrer, and I. M. Vitkovitsky, Appl. Phys. Lett. **47**, 1056 (1985).
[16] G. Schaefer, K. H. Schoenbach, M. Kristiansen, B. E. Strickland, R. A. Korzekwa, and G. Z. Hutcheson, Appl. Phys. Lett. **48**, 1776 (1986).
[17] G. Schaefer and K. H. Schoenbach, IEEE Trans. Plasma Sci. **PS-14**, 561 (1986).
[18] G. Schaefer, K. H. Schoenbach, R. A. Korzekwa, and M. Kristiansen, in *Gaseous Dielectrics V*, edited by L. G. Christophorou and D. W. Bouldin (Pergamon, New York, 1987), p. 374.
[19] S. R. Hunter, in *Gaseous Dielectrics V*, edited by L. G. Christophorou and D. W. Bouldin (Pergamon, New York, 1987), p. 363.
[20] L. G. Christophorou, D. L. McCorkle, and S. R. Hunter, in *Gaseous Dielectrics V*, edited by L. G. Christophorou and D. W. Bouldin (Pergamon, New York, 1987), p. 381.
[21] S. Arai, T. Watanabe, Y. Ishikawa, T. Oyama, O. Hayashi, and T. Ishii, Chem. Phys. Lett. **112**, 224 (1984).
[22] E. Cook, World Resources Institute, Washington, D.C., February (1995).
[23] Intergovernmental Panel on Climate Change (IPCC). The 1994 Report of the Scientific Assessment Working Group of IPCC.
[24] A. R. Ravishankara, S. Solomon, A. A. Turnipseed, and R. F. Warren, Science **259**, 194 (1993).
[25] P. Maroulis, J. Langan, A. Johnson, R. Ridgeway, and H. Withers, Semiconductor International, November, 1994, Pub. No. 325-9502.
[26] R. A. Morris, T. M. Miller, A. A. Viggiano, J. F. Paulson, S. Solomon, and G. Reid, J. Geophys. Res. **100**, 1287 (1995).
[27] A. L. McClellan, *Tables of Experimental Dipole Moments* (W. H. Freeman and Company, San Francisco, CA, 1963), p. 51.
[28] J. A. Beran and L. Kevan, J. Phys. Chem. **73**, 3860 (1969).
[29] P. Sauvageau, J. Doucet, R. Gilbert, and C. Sandorfy, J. Chem. Phys. **61**, 391 (1974).
[30] M. B. Robin, in *Higher Excited States of Polyatomic Molecules* (Academic, New York, 1974), Vol. I, pp. 178–191.
[31] C. J. Noutary, J. Res. Natl. Bur. Stand. Sec. A **72**, 479 (1968).
[32] I. G. Simm, C. J. Danby, and J. H. D. Eland, J. Chem. Soc. Chem. Commun. 832 (1973).
[33] I. G. Simm, C. J. Danby, and J. H. D. Eland, Int. J. Mass Spectrom. Ion Phys. **14**, 285 (1974).
[34] L. C. Lee, E. Phillips, and D. L. Judge, J. Chem. Phys. **67**, 1237 (1977).
[35] I. Ishii, R. McLaren, A. P. Hitchcock, K. D. Jordan, Y. Choi, and M. B. Robin, Can. J. Chem. **66**, 2104 (1988).
[36] E. Lindholm and J. Li, J. Phys. Chem. **92**, 1731 (1988).
[37] L. Lehmann, S. Matejcik, and E. Illenberger, Ber. Bunsenges. Phys. Chem. **101**, 287 (1997).
[38] T. Takagi, L. Boesten, H. Tanaka, and M. A. Dillon, J. Phys. B **27**, 5389 (1994).
[39] F. Weik and E. Illenberger, J. Chem. Phys. **103**, 1406 (1995).
[40] F. Weik, quoted in Ref. 39.
[41] T. Shimanouchi, Natl. Stand. Ref. Data Ser. (U.S., Natl. Bur. Stand.) **39**, 95 (1972).
[42] M. Hayashi and A. Niwa, in *Gaseous Dielectrics V*, edited by L. G. Christophorou and D. W. Bouldin (Pergamon, New York, 1987), p. 27.
[43] H. Okumo and Y. Nakamura, paper presented at the International Conference on Atomic and Molecular Data and Their Applications, Gaithersburg, MD, Sept. 29–Oct. 2, 1997, *Book of Abstracts*, p. 64.
[44] J. Sanabia, G. D. Cooper, J. A Tossell, and J. H. Moore, J. Chem. Phys. (in press); (private communication, 1997).
[45] O. Sueoka, H. Takaki, A. Hamada, and M. Kimura, Twentieth International Conference on Physics of Electronic and Atomic Collisions, Vienna, Austria, 23–29 July 1997; Abstracts of Contributed Papers, Vol. 1, edited by F. Aumayr, G. Betz, and H. P. Winter, Paper WEO57.
[46] P. Pirgov and B. Stefanov, J. Phys. B **23**, 2879 (1990).
[47] M. S. Naidu and A. N. Prasad, J. Phys. D **5**, 983 (1972).
[48] H. B. Milloy, R. W. Crompton, J. A. Rees, and A. J. Robertson, Aust. J. Phys. **30**, 61 (1977).
[49] F. E. Spencer and A. V. Phelps, *Proceedings of the 15th Symposium on Engineering Aspects of Magnetohydrodynamics* (University of Pennsylvania Press, Philadelphia, PA, 1976).
[50] R. Merz and F. Linder (private communication, September 1997).
[51] A. Mann and F. Linder, J. Phys. B **25**, 533 (1992).
[52] L. G. Christophorou, P. G. Datskos, and J. G. Carter, Chem. Phys. Lett. **186**, 11 (1991).
[53] R. A. Morris, C. J. Patrissi, D. J. Sardella, P. Davidovits, and D. L. McFadden, Chem. Phys. Lett. **102**, 41 (1983).
[54] H. T. Davis and L. D. Schmidt, Chem. Phys. Lett. **16**, 260 (1972).
[55] H. U. Poll and J. Meichsner, Contrib. Plasma Phys. **27**, 359 (1987).
[56] M. M. Bibby and G. Carter, Trans. Faraday Soc. **59**, 2455 (1963).
[57] M. V. Kurepa, 3rd Czechoslovakian Conference on Electronics and Vacuum Physics Transactions, Prague, 23–28 September 1965, pp. 107–115.
[58] J. A. Beran and L. Kevan, J. Phys. Chem. **73**, 3866 (1969).
[59] D. Rapp and P. Englander-Golden, J. Chem. Phys. **43**, 1464 (1965).
[60] Y.-K. Kim (private communication, 1997).
[61] Y.-K. Kim and M. E. Rudd, Phys. Rev. A **50**, 3954 (1994); W. Hwang, Y.-K. Kim, and M. E. Rudd, J. Chem. Phys. **104**, 2956 (1996).
[62] H. F. Winters and M. Inokuti, Phys. Rev. A **25**, 1420 (1982).
[63] S. Motlagh and J. H. Moore (private communication, September 1997).
[64] I. M. Bortnik and A. A. Panov, Sov. Phys. Tech. Phys. **16**, 571 (1971).
[65] S. R. Hunter, J. G. Carter, and L. G. Christophorou, J. Chem. Phys. **86**, 693 (1987).
[66] S. E. Božin and C. C. Goodyear, Br. J. Appl. Phys. **1**, 327 (1968).
[67] J. G. Carter, S. R. Hunter, and L. G. Christophorou, in *Gaseous Dielectrics V*, edited by L. G. Christophorou and D. W. Bouldin (Pergamon, New York, 1987), p. 47.
[68] W. W. Byszewski, M. J. Enright, and J. M. Proud, in *Gaseous Dielectrics IV*, edited by L. G. Christophorou and M. O. Pace (Pergamon, New York, 1984), p. 53.
[69] W. W. Byszewski, M. J. Enright, and J. M. Proud, in *Gaseous Dielectrics IV*, edited by L. G. Christophorou and M. O. Pace (Pergamon, New York, 1984), p. 255.
[70] L. G. Christophorou, R. A. Mathis, S. R. Hunter, and J. G. Carter, in *Gaseous Dielectrics V*, edited by L. G. Christophorou and D. W. Bouldin (Pergamon, New York, 1987), p. 88.
[71] L. G. Christophorou, R. A. Mathis, S. R. Hunter, and J. G. Carter, J. Appl. Phys. **63**, 52 (1988).
[72] W. A. Wilson, J. H. Simons, and T. J. Brice, J. Appl. Phys. **21**, 203 (1950).
[73] G. Biasiutti, in *Gaseous Dielectrics III*, edited by L. G. Christophorou (Pergamon, New York, 1982), p. 174.
[74] R. E. Wootton, S. J. Dale, and N. J. Zimmerman, in *Gaseous Dielectrics II*, edited by L. G. Christophorou (Pergamon, New York, 1980), p. 137.
[75] D. R. James, L. G. Christophorou, and R. A. Mathis, in *Gaseous Dielectrics II*, edited by L. G. Christophorou (Pergamon, New York, 1980), p. 115.
[76] G. Camilli, T. W. Liao, and R. E. Plump, Trans. AIEE **74** (Pt I), 637 (1955).
[77] K. Nakanishi, L. G. Christophorou, J. G. Carter, and S. R. Hunter, J. Appl. Phys. **58**, 633 (1985).
[78] G. F. Reinking, L. G. Christophorou, and S. R. Hunter, J. Appl. Phys. **60**, 499 (1986).
[79] L. G. Christophorou, *Atomic and Molecular Radiation Physics* (Wiley-Interscience, New York, 1971), Ch. 2.
[80] S. S. Nagra and D. A. Armstrong, Can. J. Chem. **53**, 3305 (1975).
[81] H. C. Sun, V. Patel, E. A. Whittaker, B. Singh, and J. H. Thomas III, J. Vac. Sci. Technol. A **11**, 1193 (1993).
[82] K. Miyata, M. Hori, and T. Goto, J. Vac. Sci. Technol. A **14**, 2343 (1996).
[83] S. R. Hunter and L. G. Christophorou, J. Chem. Phys. **80**, 6150 (1984).
[84] S. M. Spyrou and L. G. Christophorou, J. Chem. Phys. **82**, 2620 (1985).
[85] R. W. Fessenden and K. M. Bansal, J. Chem. Phys. **53**, 3468 (1970).

[86]F. J. Davis, R. N. Compton, and D. R. Nelson, J. Chem. Phys. **59**, 2324 (1973).
[87]P. W Harland and J. L. Franklin, J. Chem. Phys. **61**, 1621 (1974).
[88]S. M. Spyrou, I. Sauers, and L. G. Christophorou, J. Chem. Phys. **78**, 7200 (1983).
[89]K. A. G. MacNeil and J. C. J. Thynne, Int. J. Mass Spectrom. Ion Phys. **2**, 1 (1969).
[90]J. W. Coomber and E. Whittle, Trans. Faraday Soc. **63**, 1394 (1967).
[91]A. A. Christodoulides, D. L. McCorkle, and L. G. Christophorou, in *Electron Molecule Interactions and their Applications*, edited by L. G. Christophorou (Academic, New York, 1984), Vol. 2, Ch. 6.
[92]S. R. Hunter, J. G. Carter, and L. G. Christophorou, Phys. Rev. A **38**, 58 (1988).
[93]R. W. Crompton and R. L. Jory, Aust. J. Phys. **15**, 451 (1962).